POLITECNICO DI TORINO

Corso di Laurea Magistrale

in Ingegneria Energetica e Nucleare

Tesi di Laurea Magistrale

Simulation of enhanced efficiency of a CHP system using a High-Temperature Thermal Energy Storage

Relatori
Marco C. Masoero
William A. Ryan

Candidato
Claudia Puglisi

Anno Accademico 2018/2019

ACKNOWLEDGMENTS

First, I would like to express my gratitude to my academic advisors, William A. Ryan, for the constant support, advice and guidance, and Marco C. Masoero, for being always kind and ready to help, despite the distance. I would also like to thank Mrs. Lynn Thomas and Mrs. Jenna Stephens, for the extraordinary patience and huge efforts made to help me during the program. A special and priceless thanks goes to my beautiful family, my parents, Luca and Maria, and my siblings, Marco and Elena, for giving me such an opportunity and the unconditioned support and love. I owe you all that I have accomplished so far. Furthermore, I am beyond grateful to the person I shared the past five years with. Thanks to Angelo for always making me feel his love. A fin special thanks goes to my roommates, Hélènè, Lorenzo and Jacopo, for making my days bright and to all the people I shared this incredible journey with. You all contributed to make this experience unforgettable.

TABLE OF CONTENTS

TABLE OF CONTENTS (Continued)

CHAPTER **PAGE**

LIST OF TABLES

LIST OF FIGURES

LIST OF FIGURES (Continued)

FIGURE **PAGE**

LIST OF ABBREVIATIONS

ANSI	American National Standard Institute
ASHRAE	American Society of Heating, Refrigerating and Air Conditioning Engineers
AHU	Air Handling Unit
AWWA	American Water Works Association
CCGT	Combined Cycle Gas Turbine
CHP	Combined Heat and Power
CI	Critical Infrastructure
COP	Coefficient of Performance
CWP	Chilled Water Temperature
DHW	Domestic Hot Water
DOE	Department of Energy
EDM	Energy Design Measure
EFC	Equivalent Fuel Content
EPA	Environmental Protection agency
ERG	Exhaust Recoverable Heat
FEL	Following Electric Load

LIST OF ABBREVIATIONS (Continued)

FTL	Following Thermal Load
GHG	Greenhouse gases
HIR	Heat Input Ratio
HPR	Heat to Power Ratio
HRSG	Heat Recovery Steam Generator
HSM	Heat Storage Medium
HVAC	Heating, Ventilation and Air Conditioning
GT	Gas Turbine
LEED	Leadership in Energy and Environmental Design
MOB	Medical Office Building
NFPA	National Fire Protection Association
NREL	National Renewable Energy Laboratory
NSF	National Sanitation Foundation
PLR	Partial Load Ratio
PRSEC	Percentage Reduction in Energy Consumption
RFCW	Reliability First Corporation West
TES	Thermal Energy Storage
VAV	Variable Air Volume

LIST OF ABBREVIATIONS (Continued)

WHRS	Waste Heat Recovery System
WRH	Waste Recoverable Heat

SUMMARY

The primary goal of this work is to simulate and analyze different solutions to fulfill, with the same system, both the thermal and electric energy demand of a health care facility located in Chicago. This kind of systems are referred to as "Combined heat and power" or "Cogeneration" if they provide electricity and heat, and "Combined cooling, heating and power" or "Trigeneration" if they also provide cooling. In order to do so, the DOE software eQuest® is used to model the building and the plant which has a gas turbine as a prime mover. To provide a further improvement in the efficiency of the system, a High-Temperature Thermal Energy Storage is modeled and optimized.

The exploitation of this technology is extremely useful in reducing the energy consumption of the facility, which, in the base model, is assumed to purchase from the grid all the electricity and natural gas needed to satisfy its loads. In particular, compared to a separated generation plant, the adoption of a cogenerative system allows a wiser utilization of the energy source and enables to reduce the fuel consumed by the boiler as well as the electricity bought from the grid.

After a preliminary evaluation of the electricity and heat profiles of the building, the prime mover is modeled and a first analysis of the new consumption is conducted. In order to further increment the heat recovered by the system, the thermal storage is then added. Finally, an absorption chiller is introduced in the model to enable a better exploitation of the heat recovered and stored in the summer and, at the same time, to reduce the electric need to run the traditional electric chillers.

CHAPTER 1

CHP IN HEALTH CARE FACILITIES

The subject of this thesis is a large health care facility located in Chicago. Hospitals are extremely suitable for CHP applications for several reasons. They usually operate continuously every day of the year, 24 hours a day, requiring a large simultaneous amount of heat, cool and electricity [1]. As a consequence of that, the investment costs pay back quicker than facilities with more discontinuous loads. Another reason that makes CHP an attractive technology in the health care field lays in its high reliability. The possibility of on-site electric production reduces the dependence from the grid, improving the safety of the system in case of emergency outages. This is extremely important considering that hospitals are classified as *critical infrastructures* (CI) [2]. A critical infrastructure is defined by the U.S Department of Homeland Security as a facility whose activity, networks and systems are of vital importance for the security, economy and public health of the country.

1.1 The base model

In order to run the simulations for the CHP system, a model of a building that is representative of an average American hospital needs to adopted. In this study, this is done by implementing on eQuest® the data and features of the hospital model developed by the National Renewable Energy Laboratory (NREL)[3] in compliance with the ANSI/ASHRAE Standard 90.1-2004[4]. The location of the building is Chicago, IL that, according to the standard

ASHRAE 169-2006 [5], is part of the climate zone 6A which defines the cold-humid climates. The prototype has a total floor area of 527,000 [ft^2] that accounts for a 427,000 [ft^2] seven-story hospital building and for a 100,000 [ft^2] five-story medical office building (MOB). The glazed area is not explicitly available but it can be estimated by knowing the floor-to-floor height (10 ft) and the heights from the floor to the bottom of the window and from the top of the window to the ceiling (respectively 3.6 ft and 2.4 ft). Considering that the windows follow the perimeter of the building without any opaque interruptions, the ratio between glazed and opaque area is 40%. A picture of the hospital prototype is provided in Figure 1.

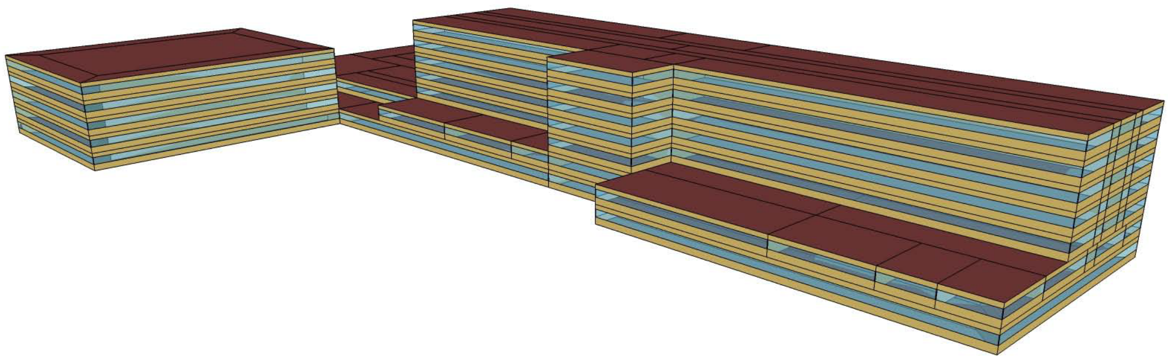

Figure 1: Hospital prototype view from Southeast

The prototype is designed to provide a set of measures that allow the building to achieve, independently on the climate zone, the target of 50% reduction in energy consumption. Some of these Energy Design Measures (EDMs) used by the NREL consisted in reducing the power density of the lighting system and introducing in the suitable zones daylighting control and occupancy sensors. As far as the envelope is concerned, the insulation layer is increased and the envelope itself is made tighter to reduce infiltration. Free gains are handled by putting overhangs on the windows facing south and high-efficient equipment (boilers, heaters, chillers and pumps) has to be installed.

The heating, ventilation and air-conditioning system in the prototype is equipped with boilers, electric chillers, a central air handling unit (AHU) provided with hot and chilled water coils and a final unit with reheat coils. These characteristics are only valid for the *base model* as, in order to optimize it, the CHP or CCHP system will require to install new equipment to enable the heat recovery to run the hot water loop and chilled water loop.

The model of the prototype was implemented, validated and improved in previous works [6][7]. The improvement of the model was necessary as the base one showed some flaws related to the temperature in some of the spaces. In fact, the thermostat in these spaces revealed that the temperature was below the set-point for a relevant fraction of the year. This error was addressed by manually introducing pre-heat coils in every Variable Air Volume HVAC system, ensuring a correct operation of the plant, especially in the winter season. This is extremely important as the temperature of the air entering the system in winter, is likely to be lower than water freezing temperature. As a consequence of that, it is possible for the water inside the cold deck coils to freeze rising the risk of damaging the coils themselves. The other intervention made in the eQuest® model concerns one of the coils parameter, the *Reheat Delta T*. This number, set to 30 [F] in the default layout represents the maximum temperature increase that the supply air undergoes while crossing the reheat coils. To ensure that air is supplied at the correct temperature, the specification *Reheat Delta T* is brought up to 50 [F]. Since these two measures where shown to be insufficient to guarantee all spaces to reach the set-point temperature, a third and last one is implemented. In this case a parameter called *sizing ratio*, used to undersize or oversize the equipment, is modified from 1 to 1.15 in the spaces that still showed an under heating [7]. In particular the *sizing ratio* is a multiplier for the coil size and air-flow rate values calculated by the software. The combination of these three techniques allows all spaces to reach the desired temperature.

1.2 Energy profiles

The first step before modifying the layout of the plant, is to analyze the performances of the *base model*. This means running a simulation on eQuest®, that provides as outputs the hour-by-hour consumption of electricity, fuel and heat. These values can be elaborated using a spreadsheet in order to obtain a graphic representation of the profiles. It is worthy of noticing that the fuel demand that is here reported, accounts for the thermal needs of the building, which are space heating and domestic hot water, but also for other equipment that require a certain amount of fuel throughout the year, like kitchens and laundries. It is, however, more meaningful to perform all the analysis on the fuel demand rather than on the thermal load of building, as the latter is not influenced by how the thermal energy is generated. The fuel profile, instead, accounts for the conversion efficiency of the system, giving the chance of appreciating the differences in fuel consumption when using different generation methods. The hourly electric load of the building, in [MW], throughout the 8760 hours of the year is represented in Figure 2.

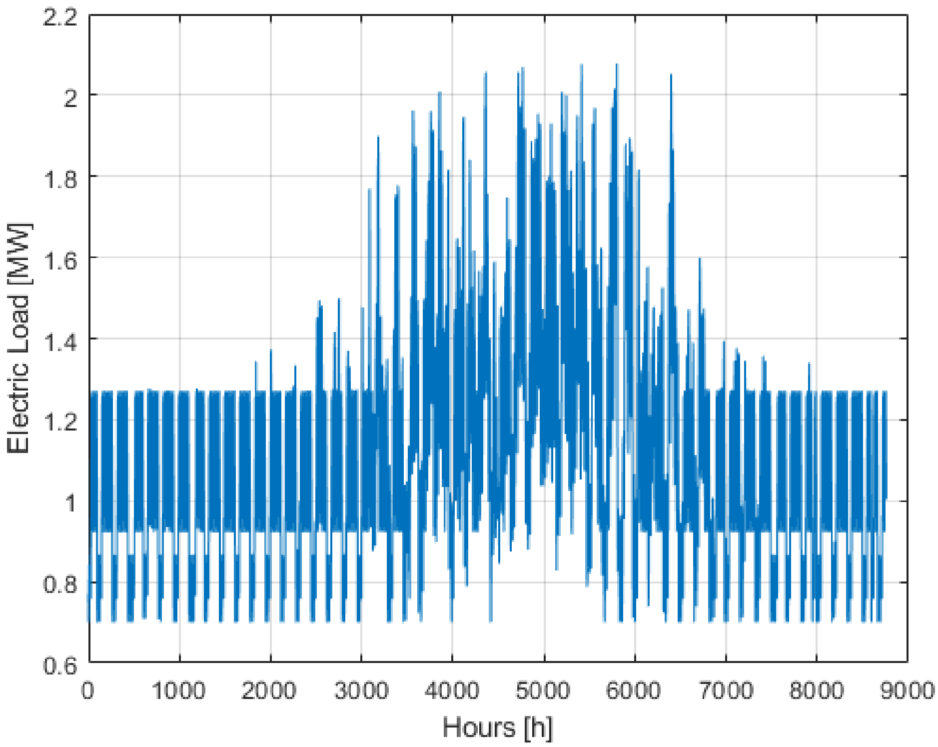

Figure 2: Base model annual electric consumption

The profile shows fluctuations between 700 [kW] and 1.3 [MW] during the heating season, given by the daily occupation of the building and by the use of the equipment. The cooling season, instead, is also characterized by the use of three electric chillers that bring the electric consumption to a substantial increase in the peak load, reaching 2.1 [MW]. The three chillers produce the chilled water needed to feed the cold deck of the AHU.

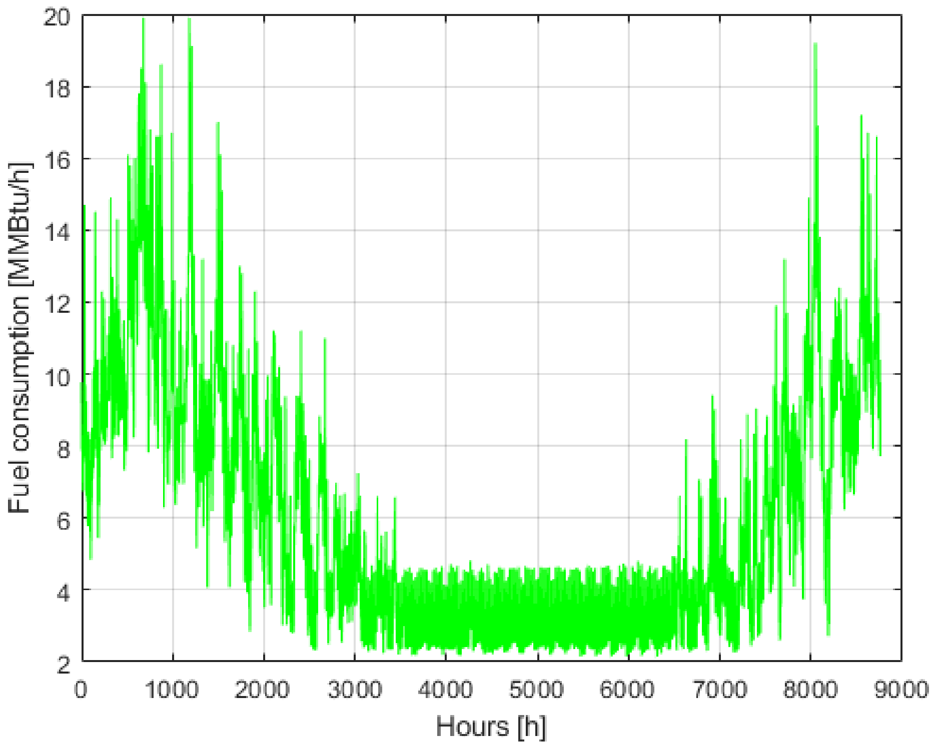

Figure 3: Base model annual fuel consumption

The fuel consumption profile (Figure 3) has an opposite trend compared to the electric one. It comprises the fuel consumption for space heating, domestic hot water and, finally, the fuel needed for activities like cooking, washing and drying. In this case, summer months are those that require less space heating, it is thus possible to notice a stable fluctuation between 2.1 [MMBtu/hr] and 4.8 [MMBtu/hr]. In winter, especially between January and February, peaks of 20 [MMBtu/hr] are reached.

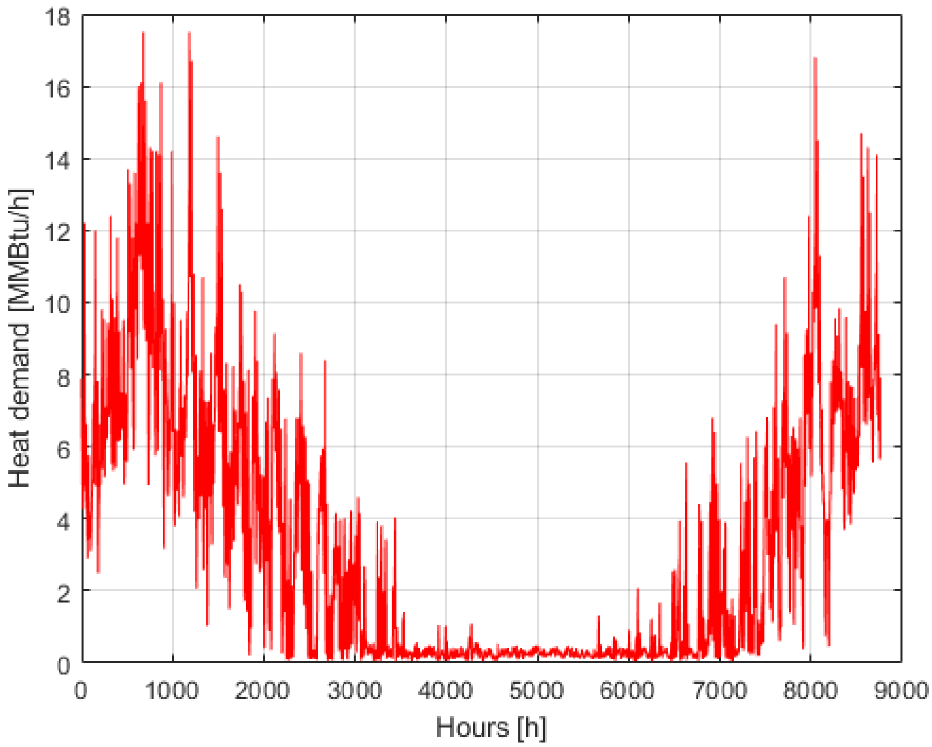

Figure 4: Base model annual heat demand

The profile of the facility heating load (Figure 4) follows the same trend of the fuel one but, obviously, differs in terms of magnitude as it does not keep in consideration the conversion efficiency of the system. In addition, this profile does not allow to distinguish between the heat needed for the purpose of space heating and for that needed for the domestic hot water.

These profiles, although useful to understand the facility needs throughout the year, do not give enough information for sizing the system. In order to do so, a different kind of graph could be used, a *duration graph*. A *duration graph*, represents the number of hours for which a certain load persists. The y-axis shows the magnitude of the load, while the x-axis the number of hours of the year. As a consequence of that, a *duration curve* will always be a decreasing curve, that has the peak load as the maximum (usually for a negligible number of hours) and the base load as the minimum. The latter persists for 8760 hours, meaning that, for the whole year, the load is always at least equal to this number. The duration curves for the fuel and electric consumption are shown in Figure 5 and Figure 6.

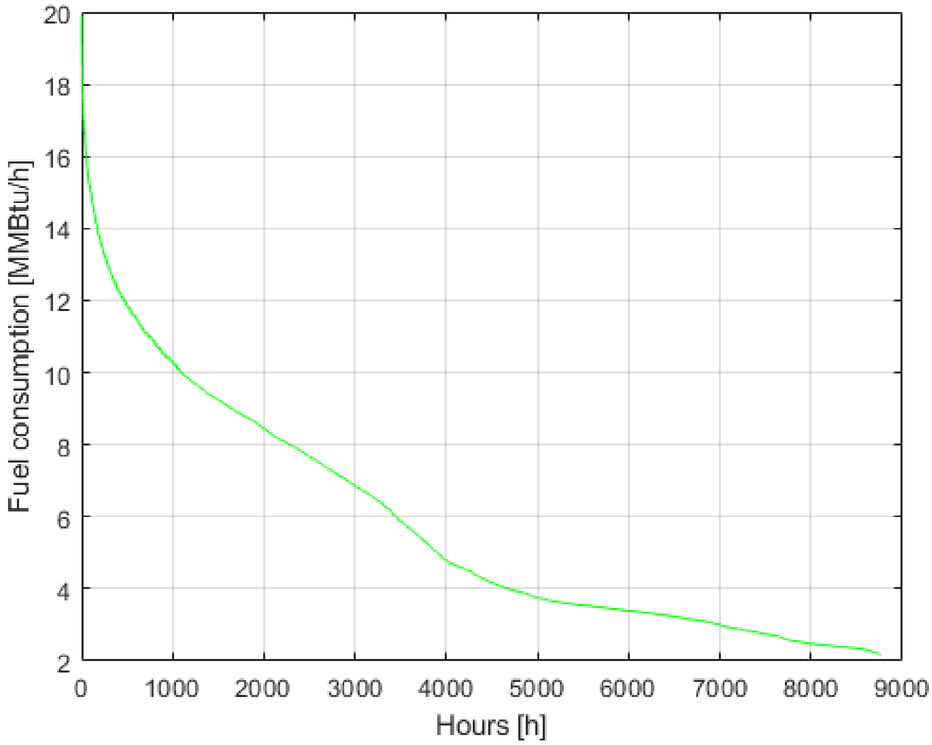

Figure 5: Base model annual fuel duration curve

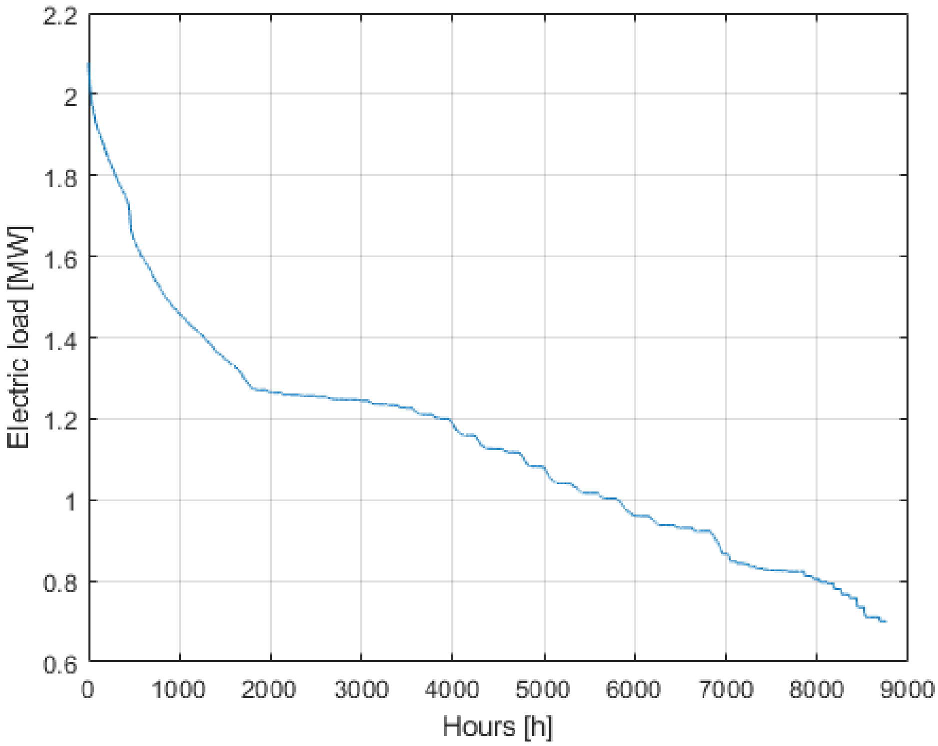

Figure 6: Base model annual electric duration curve

CHAPTER 2

THE GAS TURBINE

2.1 Introduction

Today, gas turbines are one of the most widespread technologies in the power generation industry. The idea behind them has to credited to John Barber who, in 1791, patented the first gas turbine in his work "A Method of Rising Inflammable Air for the Purposes of Procuring Motion". However, it nearly took 150 year of research and experimentation before the first actual industrial gas turbine was launched on the market by the Swiss company Brown Boveri[8]. It is thus from the 1930s that this technology started growing, improving and spreading the market to the point that today units from 500 [kW] up to 490[MW] are commonly commercialized. The efficiencies of these equipment have also experienced an outstanding growth, going from around 17 % to more than 40% [8]. On the other hand, much smaller and compact units, in the size range from 25 [kW] to 500 [kW], referred to as *Micro turbines* [9], are starting to become popular. They can be extremely advantageous for some application, including cogeneration, however, *micro turbines* will not be part of this study.

Gas turbines can be part of different plant layouts; it can thus be useful for the goal of this study to classify the main options. The most straight forward is the simple cycle layout, that has electric power as its only output[7]. Alternatively, cogeneration plants can be also found. According to a strict definition of CHP system, this is a system that exploits the thermal energy in the exhaust gases for a direct use. Examples of direct use are space heating, drying processes and the production of hot water or steam in a device like a *heat recovery steam generator* (HRSG). Nevertheless, if the HRSG is used to run a steam turbine for power generation, this configuration is more properly called *waste heat to power* (WHP) or *combined cycle* (CCGT); although, some studies still consider WHP a form of cogeneration[7].

Combustion turbines were initially meant only for power generation and, today, *single cycle gas turbines* still account for 32% (315 [GW]) of the entire U.S. power plant capacity and satisfy the peak loads. However, thanks to their high temperature exhaust gases, gas turbine cover almost 40 [GW] (around 50%) of the entire WHP U.S capacity, [6] . The reason behind the popularity of CCGT plants lays in the much higher efficiency of the system compared to other technological solutions; as of today, efficiencies higher than 60% have been reached. Because of that, the electric output delivered to the grid is maximized.

The use of combustion turbines for cogeneration is attractive for many reasons. The first one is their reliability; in fact, modern GT can run continuously up to 50,000 hours with the proper maintenance. This feature is of extreme importance especially for facilities, like hospitals, where an electric outage could have fatal consequences. Energy independence is thus a key factor in health care facilities; for this reason on-site power generation is often chosen. Moreover, GT can be driven by a large number of different fuels, mainly gaseous. Most commonly, natural gas is used and a backup of liquid fuel is kept to ensure reliability and to buy natural gas at its lowest rates. Natural gas is also considered one of the cleanest fossil fuels currently on the market, because of its low CO2 emission. Considering that GT often come with a lean premixed burner that allows to reach extremely low emission values, an environmental benefit is featured as well. In fact, these burners, also known as *dry low-NOx combustors*, can guarantee NOx emissions lower than 25 [ppm] and CO emissions between 10 and 50 [ppm] at the same time. The addition of a *selective catalytic combustion* step can then further improve the performances by taking the NOx emission down 9 [ppm] and below.

2.2 The working cycle

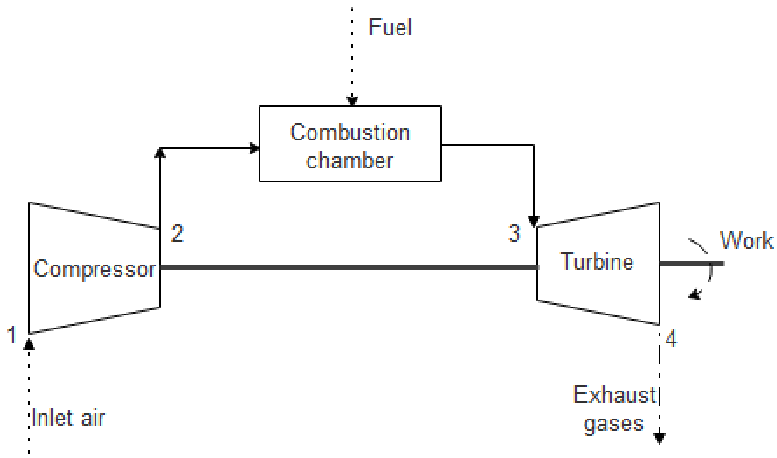

Figure 7: Gas turbine scheme

When talking about combustion turbines, reference is usually made to the complex of a compressor, a combustor and a turbine. A schematic representation of the whole equipment is give in Figure 7.

These three components work together following a thermodynamic cycle called Brayton-Joule. Although referred to as a cycle, the Brayton-Joule one in its original configuration is not strictly a cycle; the reason is that the starting point and the ending point of the process do not coincide. The transformations that characterize the Brayton-Joule cycle are the following:

1. Ambient air is compressed by the compressor up to a suitable pressure before entering the combustion chamber;
2. The pressurized air is heated in the combustion process;
3. The gas mix of air and combustion products enters the turbine and, expanding, produce the shaft work needed to drive both the electric generator and the compressor;
4. Exhaust gases are expelled.

The thermodynamic transformation of the ideal cycle on both the *pressure-volume* and *temperature-entropy* diagrams are reported in Figure 8.

The GT actually comprises two elements; the first one, called *gas producer*, is in charge of producing the mechanical power to run the compressor. The second one is the actual power module that provides the mechanical output for the electric generation.

As anticipated, this is the conventional Brayton-Joule cycle, however, many alterations and improvements can be made on it in order to raise the efficiency. As an example, by recovering

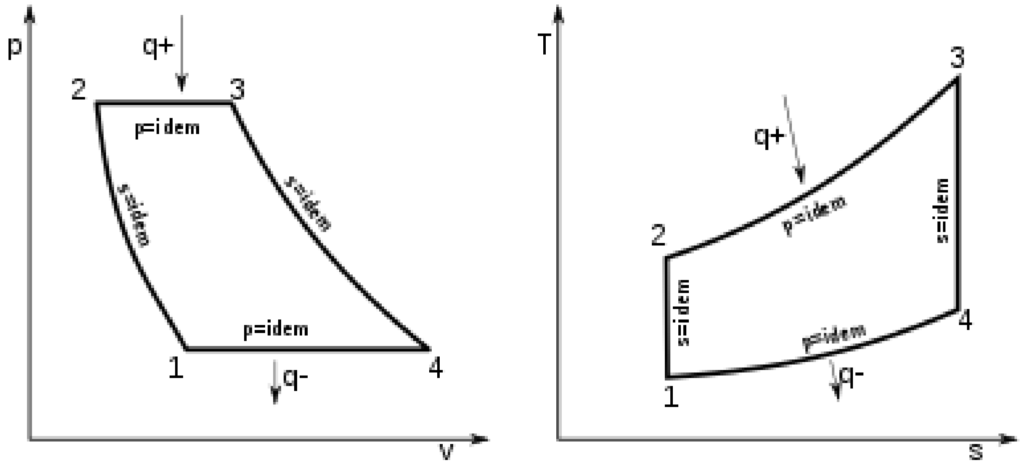

Figure 8: Ideal Brayton-Joule cycle transformation

the heat content in the exhaust gases using a regenerative heat exchanger, it is possible to preheat the air coming out from the compressor before it undergoes combustion. This technique allows to decrease the fuel consumption from the combustor and, at the same time, increase the efficiency of the system. Similarly, the efficiency can be improved by reducing the work needed by the compressor. Such work, is inversely proportional to the density of the inlet air, meaning that the colder the air the smaller is the work required. To achieve this goal the inlet air can be either pre-cooled or cooled down during the compression process using a multistage compressor with inter-coolers. A scheme of the system provided with a regenerative heat exchanger and inter-coolers is shown in Figure 9.

The efficiency of the ideal thermodynamic cycle, i.e. the cycle where the compression and the expansion are considered isoentropic, can be calculated as shown in the Equation 2.1.

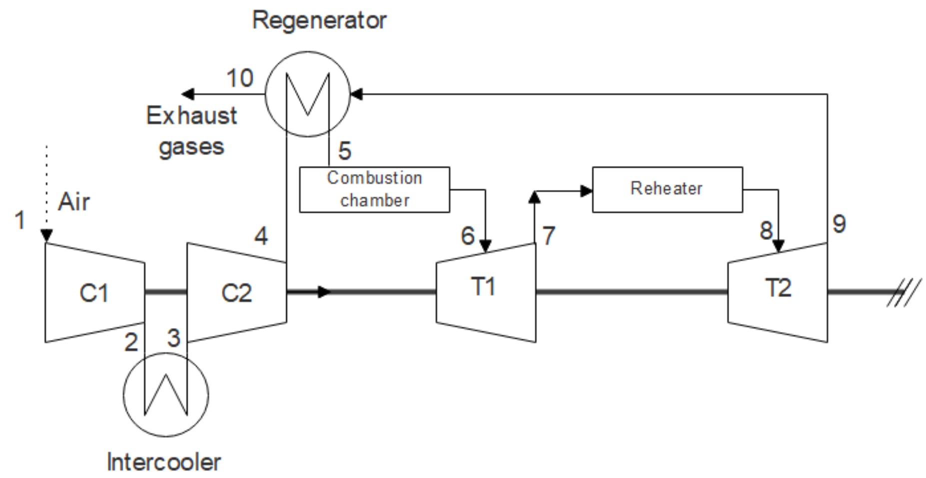

Figure 9: Scheme of a gas turbine equipped with regenerative heat exchangers and inter-cooler

$$\eta = 1 - \frac{T_D}{T_C} = 1 - \frac{1}{\rho^{\frac{\gamma-1}{\gamma}}} \tag{2.1}$$

- η Overall efficiency of the cycle;
- T_D Absolute Temperature of the exhaust gases at the outlet of the power generation section of the turbine;
- T_C Absolute Temperature of the exhaust gases at the admission to the turbine;
- ρ Turbine pressure ratio ($\rho = \frac{p_C}{p_D}$);
- γ Air specific heat ratio ($\gamma = \frac{c_p}{c_v} = 1.4$ in standard conditions);

Analyzing Equation 2.1, it is immediate to understand the influence of the gas inlet and outlet temperatures on the efficiency of the equipment. Increasing T_C, especially, gives a strong contribution in improving the efficiency. However, it is a technical challenge to raise this value, mainly due to constraints connected with the materials in the first stages of the the turbine. One common solution to make the blades both resistant to high temperatures and corrosion (that is enhanced in hot environments), is to use special metallic alloys coated by a thin layer of a ceramic material[10]. Again, the Mitsubishi Hitachi M701J is among the most advanced machines on the market, operating with an inlet temperature of 2,912 [F]. The other technique used, together with the temperature rise, is the pressure ratio enhancement.

2.2.1 Partial load operation

An important feature of gas turbines is that their power output can be controlled based on the facility actual need. This operation strategy is referred to as *partial load operation* and usually consists in reducing the fuel mass flow rate sent to the burner. However, a reduction in fuel consumption causes the amount of heat provided to the gas to decrease and, as a consequence of that, the gases inlet temperature in the turbine decreases as well, lowering the efficiency of the system. Oversizing the prime mover leads to higher number of hours throughout the year at part load, with detrimental effects on the efficiency, thus, on the economy and convenience of the plant.

Partial load operations can be mathematically described by making some assumptions. First the gases are considered to be ideal, meaning that their specific heat is constant. The cycle, thus all the components are also regarded as ideal, so the transformations are isentropic and the heat losses to the environment are assumed to be negligible. Under these hypothesis the turbine power output can be formulated and modified as follow:

$$P = (G_a + G_f) \cdot l_t - G_a \cdot l_c = \tag{2.2}$$

$$P = (G_a + G_f) \cdot c_p \cdot (T_C - T_D) - G_a \cdot c_p \cdot (T_B - T_A) = \tag{2.3}$$

$$P = (G_a + G_f) \cdot c_p \cdot T_C \cdot \Big(1 - \frac{T_D}{T_C}\Big) - G_a \cdot c_p \cdot T_A \cdot \Big(\frac{T_B}{T_A} - 1\Big) = \tag{2.4}$$

$$P = (G_a + G_f) \cdot c_p \cdot T_C \cdot \Big(1 - (\frac{p_C}{p_D})^{\frac{1-\gamma}{\gamma}}\Big) - G_a \cdot c_p \cdot T_A \cdot \Big((\frac{p_B}{p_A})^{\frac{\gamma-1}{\gamma}} - 1\Big) = \tag{2.5}$$

$$P = (G_a + G_f) \cdot c_p \cdot T_C \cdot \Big(1 - \beta_t^{\frac{1-\gamma}{\gamma}}\Big) - G_a \cdot c_p \cdot T_A \cdot \Big(\beta_c^{\frac{\gamma-1}{\gamma}} - 1\Big) = \tag{2.6}$$

$$P = (G_a \cdot c_p) \cdot \left(\left(\frac{1+\alpha}{\alpha}\right) \cdot T_C \cdot \Big(1 - \beta_t^{\frac{1-\gamma}{\gamma}}\Big) - T_A \cdot \Big(\beta_c^{\frac{\gamma-1}{\gamma}} - 1\Big)\right) = \tag{2.7}$$

- P Gas turbine power output;
- l_c Compressor work input;
- l_t Gas turbine work output;
- G_a Air mass flow rate;
- G_f Fuel mass flow rate;
- c_p Specif heat of the gas at constant pressure;
- β_c Compressor pressure ratio $\beta_c = \frac{p_B}{p_A}$;
- β_t Turbine pressure ratio $\beta_t = \frac{p_C}{p_D}$;

- α Air to fuel ratio $\alpha = \frac{G_a}{G_f}$.

The main steps to go from Equation 2.2 to Equation 2.7 consist in writing the compressor and turbine works as a function of the temperatures and then applying the equation for the isentropic transformation. Finally the air mass flow rate is highlighted and the dimensionless parameter *air to fuel ratio* is introduced. Equations 2.2 to 2.7 also show the direct dependence of the power output from the temperature T_C. The higher T_C the bigger the work produced by the turbine and, as a consequence,the power out output.

Another consequence of the part load operation, is the increase in the emission of pollutants that becomes particularly critical when the ratio between the actual and the design power outputs,called*part load ratio* (PLR), is closer or lower then 50%. The PLR is defined as follows:

$$PLR = \frac{\text{Current Power Output } [P_C]}{\text{Full Load Power output } [P_{FL}]} = \%FullLoad \tag{2.8}$$

2.3 Gas turbine model on eQuest®

After analyzing the base model of the hospital, the prime mover, in this case the gas turbine, has to be added in order to start building the CHP system objective of this study. Although eQuest® already has a native turbine model[11], this was shown to be extremely obsolete, compared to actual turbines used today. Some improvements were done to the performance curves describing the turbine behaviour by Cicciarella in [7] and Romano in [12] . The improvement of the turbine model is not the main scope of this study, however, due to the inconsistency of the results in the previous works, the main steps of the procedure have been here repeated to obtain more accurate and reliable results.

When defining the turbine properties, eQuest® requires to define three curves describing:

- The *heat input ratio* with respect to the PLR;
- The *capacity* with respect to the *heat input ratio*;
- The *exhaust heat recovered* with respect to the PLR.

In this study, the two main adjustments were aimed to modify the first two curve curves, while the third one is kept unmodified (so the eQuest® default curved is used). The data used from now on are provided by the manufacturer SOLAR Turbines ®and refer to the turbine model Taurus 60™[13][14]. Although this model is oversized for the needs of the facility, being a 5 [MW] turbine, it was chosen over a smaller turbine (like the 1[MW] Saturn 20™). The reason for that is that the Saturn 20™, despite its more suitable size, would not be representative of currently used turbines on the market, as it is extremely obsolete.

2.3.1 PLR performance curve

The first curve required by eQuest® describes the behaviour of a parameter called *heat input ratio* (HIR) when varying the PLR[11]. The HIR is defined as follows:

$$HIR = \frac{\text{Heat supplied at current conditions}}{\text{Heat supplied at Full Load}} = \frac{\frac{P_C}{\eta_C}}{\frac{P_{FL}}{\eta_{FL}}} = \eta_{FL} \cdot \frac{P_C}{P_{FL} \cdot \eta_C} = \eta_{FL} \cdot \frac{PLR}{\eta_C} \tag{2.9}$$

- η_C Efficiency of the system at current condition
- η_{FL} Efficiency of the system at full load

The *HIR vs PLR* curve is obtained by initially building a relationship describing the efficiency trend with respect to the partial load ratio by plotting and interpolating, with a quadratic relationship, the points provided by the SOLAR Turbines® technical manual[13]. Following the prescription of the manufacturer on the lowest power output for a safe operation of the equipment, the PLR varies from 10% to 100%. The improvement of the eQuest® model allows the full load efficiency to grow from less than 20% to almost 30%. The two efficiency formulations are reported in Equation 2.10 and 2.11 and graphically represented in Figure 10.

$$\eta_{eQuest} = (2.98E - 4)x^2 + (7.56E - 2)x + 8.42 \tag{2.10}$$

$$\eta_{SOLAR} = (-2.61E - 3)x^2 + 0.464x + 8.52 \tag{2.11}$$

Using the Equation 2.11 in Equation 2.9, two expressions for the HIR as a function of PLR are found (Equation 2.13 and 2.14), where x is the PLR. eQuest® requires as input the coefficients of the curve in the form:

$$HIR = a + bx + cx^2 \tag{2.12}$$

$$HIR_{SOLAR} = 0.1728 + 0.7784x + 0.0278x^2 \tag{2.13}$$

$$HIR_{SOLAR} = 0.0493 + 1.7825x - 0.8432x^2 \tag{2.14}$$

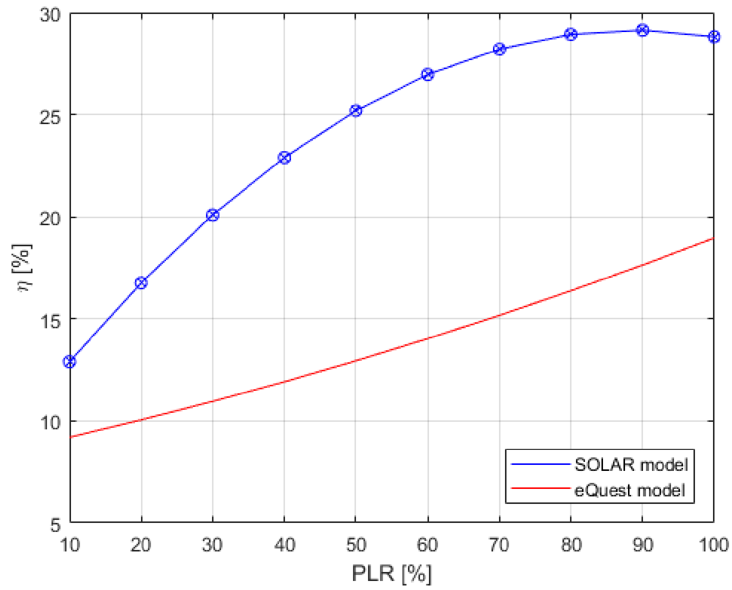

Figure 10: Efficiency behaviour as a function of the Part Load Ratio

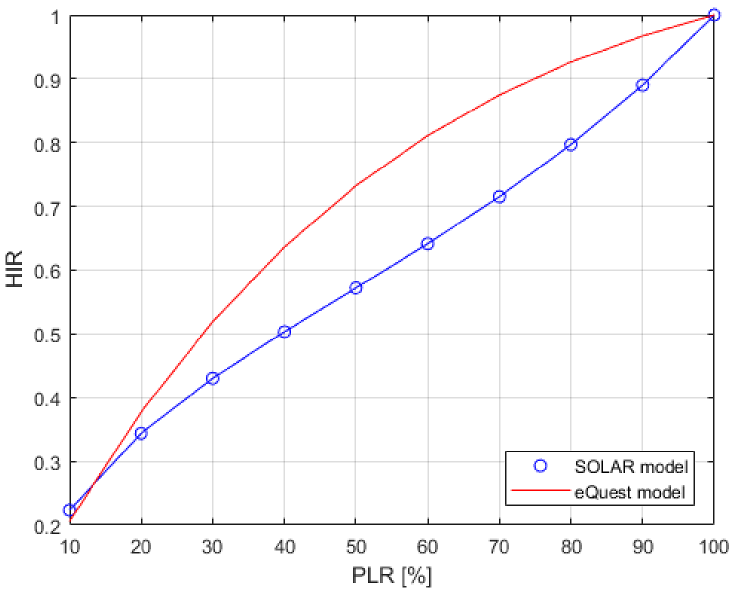

Figure 11: Heat Input ratio as a function of the Part Load Ratio

2.3.2 Temperature performance curve

To properly run the turbine model, another curve describing the variation of the efficiency with respect to the outdoor temperature is required. This curve is erroneously referred to as *Capacity* as a function of HIR, however previous works [7][12] demonstrated that the software requires a relationship between external temperature and efficiency instead. As shown in Equation 2.5, both the external temperature and atmospheric pressure have a strong effect on the power out, and on the efficiency as a consequence. However, as the equipment does not change its elevation, the effect of the pressure is neglected. An increase in the air inlet temperature causes a reduction in the air density that leads to two negative effects on the system. First, the air mass flow rate decreases and, as demonstrated in Equation 2.7, the power output is directly proportional to G_a. Moreover, since the compression work is proportional to the specific volume of the gas, l_c increases causing the power output to further reduce. In order to deal with these issue, the *International Standard Organization* (ISO) set some reference conditions for the evaluation of GT performances[15]. The reference temperature was set to 59[F] while the pressure was chosen equal to the sea level one, 101,325[Pa]. By using the data provided the manufacturer, the power output grows to 105% of the one estimated with the ISO standard when the temperature is brought to 50[F] and goes down to 90% when the outdoor temperature approaches 100[F].

The curve required by eQuest® has a linear trend and is in the following form.

$$\eta_{\%} = a + bx \tag{2.15}$$

Where x is the outdoor temperature. The two linear curves obtained from eQuest® and the SOLAR® data-sheets are reported in Equation 2.16 and 2.17, and graphically in Figure 12.

$$\eta_{\%eQuest} = 124 - 0.41x \tag{2.16}$$

$$\eta_{\%SOLAR} = 114.6 - 0.24x \tag{2.17}$$

A more realistic trend for this curves would reach a plateau, approaching a 100% capacity,

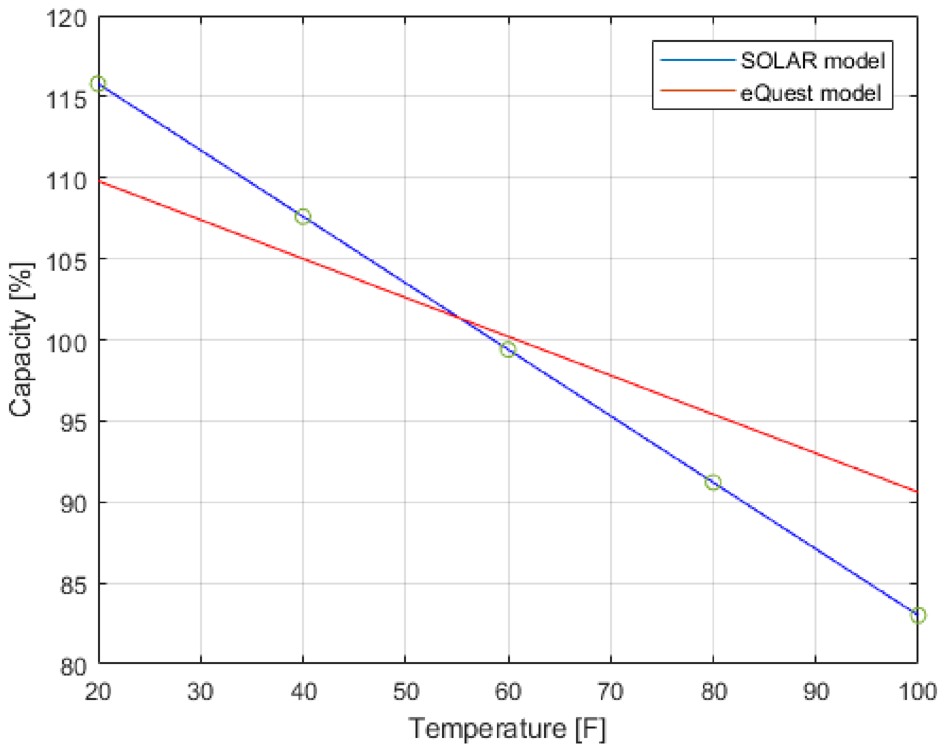

Figure 12: Effect of external air temperature on the gas turbine capacity

below a temperature of around 59[F]. However, this is not mathematically feasible as eQuest® forces the performance curve to have a linear trend.

2.3.3 Recoverable heat curve

The last performance curve describes the trend of the heat recoverable from the turbine as a function of the *partial load ratio*. This one, has not been changed, so the software default curve was used. The correlation is the following:

$$ERH = 0.2956 + 0.4930x + 0.2113x^2 \tag{2.18}$$

Where x is the *partial load ratio*.

CHAPTER 3

THE COGENERATION PLANT

This chapter provides a comprehensive analysis of the electric and fuel consumption of the facility when installing a CHP system with different sizes of the prime mover. Since the ultimate goal of this study is to determine the effects of a thermal energy storage on the efficiency of the plant, a preliminary explanation and calculation of these parameters is also carried on.

3.1 Introduction to the technology

A cogeneration plant consists in a certain number of systems that work in synergy to produce an electric and thermal output at the same time. This kind of system is gaining increasing popularity thanks to its relatively high efficiency and numerous benefits. A list of the major benefits provided by the implementation of a CHP system has been elaborated by the U.S. Department of Energy (DOE) together with the U.S Environmental Protection Agency (EPA)[16]. A summary of such benefits is here reported.

- **Reliability:** the on-site electric and thermal generation could allow the facility to keep running even during catastrophic events or grid outages;
- **Reduced environmental impact:** the possibility to obtain two products from the same amount of burned fuel, reduces the emission of air pollutants and greenhouse gases;
- **High efficiency:** the amount of fuel burned to obtain the electric and thermal power is extremely reduced with respect to a traditional separated generation system. Further-

more, the on-site generation also eliminates the need for long transmission and distribution infrastructures, avoiding the related losses and costs;

- **Economically beneficial:** CHP system can prevent from increases in the electric rates and also provide a cost effective and cost saving solution for the facility it is implemented in.

Cogeneration plants are extremely suitable for applications with a high, steady and coincident electric and thermal load. Factories where highly energy demanding industrial processes are carried on, have the highest share of CHP installed capacity[16]. However, other types of buildings, e.g hospital, university campuses, hotels and commercial buildings, might also represent good opportunities for this type of technology, due to their continuous operation throughout the year and high hot water demand.

The *prime mover*, is the the cardinal element of a CHP system. It is its job to convert the chemical energy in the fuel by burning it and provide the mechanical energy required to run the electric generator. As a part of the combustion process (in the case of a reciprocating engine or a gas turbine), some thermal energy is rejected. The scope of a cogeneration system is to recover part of this rejected energy and make it available to satisfy the user's heat demand. This is usually done by a group of heat exchangers, that are referred to as *Waste Heat Recovery System* (WHRS). A correct and coordinate operation of all the equipment is guaranteed by a set of controls. As anticipated in Section 2.1 the heat content of the gases, which can be up to 80% of the energy content in the fuel, can be either directly used to produce hot water , or steam in a HRSG for steam production.

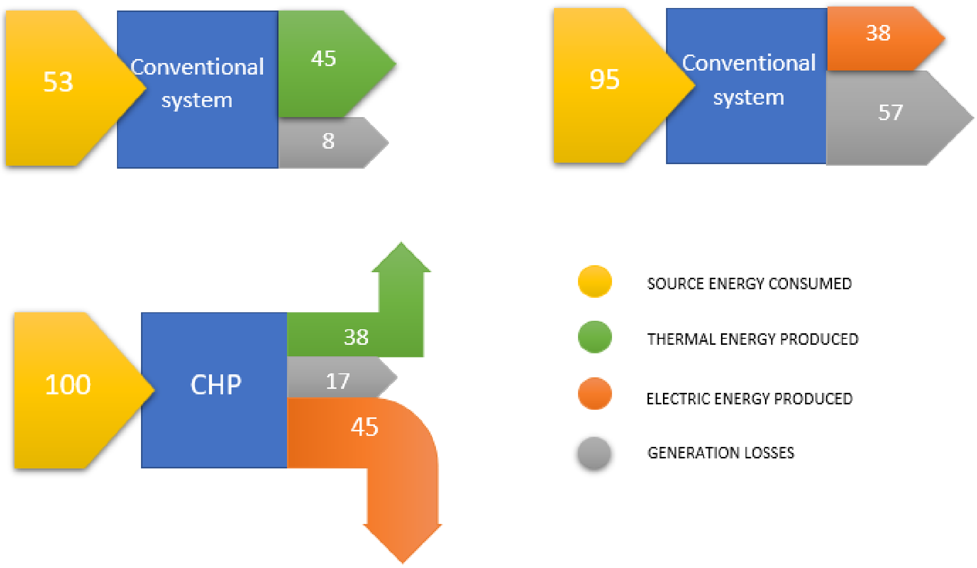

Figure 13: Energetic comparison between a CHP system and conventional separated generation system

A schematic comparison between a CHP system and a traditional separated system is provided in Figure 13, considering average values for the conversion efficiencies. Notice that, to produce the same amount of electric and thermal energy, a CHP system requires 48 units of primary energy less than a conventional generation system.

3.2 Thermal flows characterization

In order to provide the reader a full comprehension of the topic discussed later on in this study, the energy flows involved in the process need to be clarified. A graphic representation of these is provided in Figure 14 for a deeper insight. The combustion process generates a

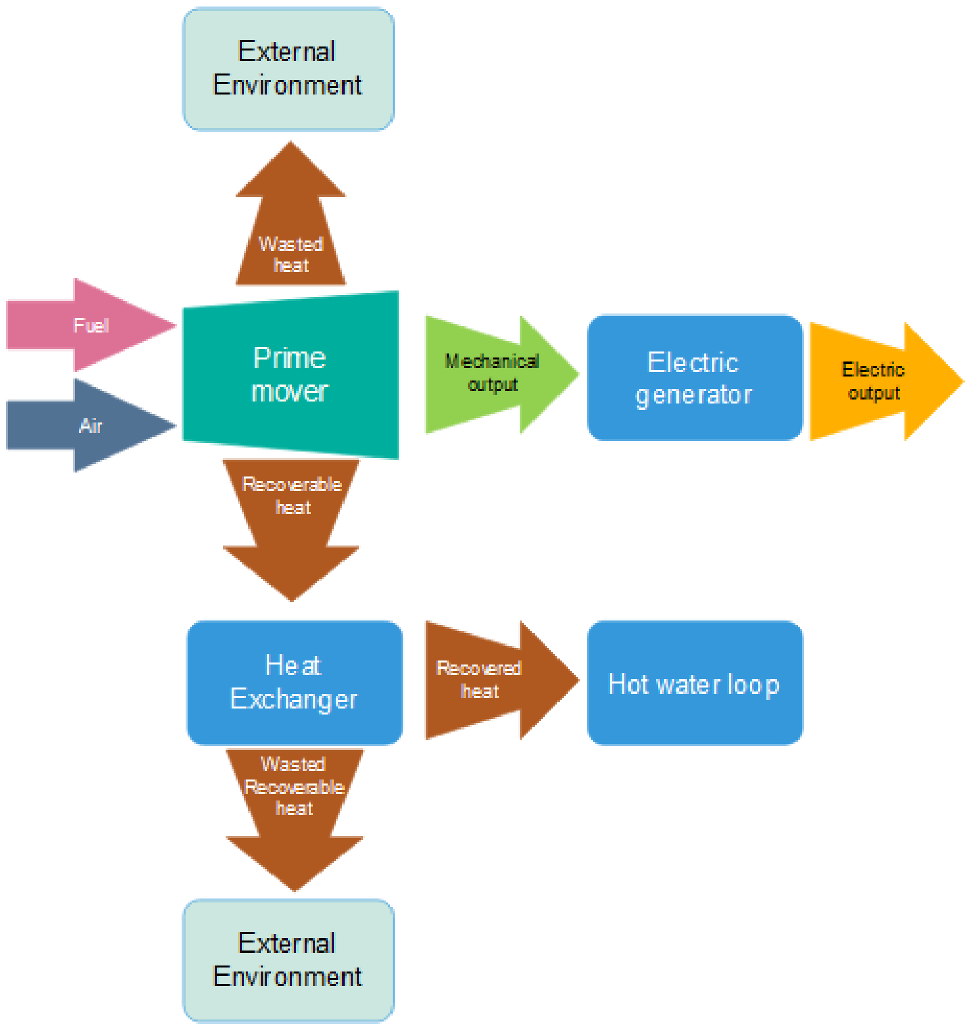

Figure 14: Energy and Mass fluxes in a cogeneration plant

certain amount of high-temperature gases that are sent to expand in the turbine. During and after the expansion (when the gases flow through the WHRS) a fraction of the heat content in the gases is inevitably released towards the surrounding environment; this thermal flux is referred to as *Wasted Heat*. The amount of heat that, instead, survives the inefficiency of the WHRS and is thus potentially usable, is called *Recoverable heat*. This energy is just potentially exploitable for two main reasons:

- The recoverable heat might not have the thermodynamic characteristics needed to meet the constraints of the system, especially in therms of temperature and pressure;
- The thermal demand profile of the facility might require the a smaller amount of energy than the recoverable heat; in this case the excess is wasted.

The *recoverable heat* can then be further divided into two thermal fluxes: the *Recovered heat* which is the amount of heat actually provided to the user, and the *Wasted recoverable heat* (WRH) which is the amount of heat that, for one of the reasons mentioned above, cannot be used. The latter, does not have to be confused with the *wasted heat* lost through the system.

3.3 Plant management strategies

As combined heat and power plant are designed to be able to produce both thermal and electric energy, it is important to explain the management strategies that can be used to run the system based on the primary need of the user. The main possible strategies are referred to as *Follow the electric load* (FEL) and *Follow the thermal load* (FTL). However some combinations of the the two can also be implemented[11]. An explanation of these techniques is here provided.

- **Following the electric load:** the primary output of the system is electricity, meaning that the prime mover provides as output the exact amount of electricity needed by the user, if this is smaller than the prime mover capacity. Otherwise, the prime mover runs full load and the difference between the electric load and output is purchased from the grid. In this case the heat produced is a secondary output, only meant to reduce the gas consumption from the boiler.
- **Following the thermal load:** the primary goal of the system is to satisfy the user thermal demand and to prevent the boilers from running. In this case the system heat output follows the thermal profile as much as possible and the electric output is a secondary product meant to reduce the amount of electricity purchased from the grid.

Other strategies, that are also possible to implement on eQuest®, require a much more delicate control as the load followed is either the smallest or biggest among the two[11]. The criteria to determine the most suitable strategy consists of calculating a parameter called *Heat to Power ratio* (HPR) that is defined as follow (with both quantities is [MWh]):

$$HPR = \frac{\text{Heat Demand}}{\text{Electric Demand}} \tag{3.1}$$

If the HPR bigger than 1, a FTL strategy would be recommended, otherwise the FEL is more suitable. This is the case of most health care facilities that, having a much higher electric load compared to the thermal one, make the FEL strategy the most appropriate. To confirm that, the HPR for the case of study here implemented, is calculated, giving a result of 58.6%. The main reason for this comparatively high electric load is the large summer consumption caused by the electric chillers. The consequence of an eventual FTL strategy would be a continuous fluctuation in the turbine operation and, because of the small summer thermal load, a partial load operation for a large amount of hours. This would result in the system running at a low efficiency or, to avoid that, in undersizing the equipment. Both alternatives are far from being cost effective. Moreover, the FEL strategy ensures a higher reliability of the system in case of emergency and power outages, that is one of the major concerns for a health care facility.

3.4 The CHP model on eQuest®

In this section the main steps and considerations made to implement the CHP system on eQuest® are explained. The design of the plant on eQuest® is fundamental to then be able to run the simulations that allow to derive the new consumption profiles of the building. By changing the size of the prime mover first, and the capacity of the TES, then, it will be possible to determine the optimal size of both to maximize the performances of the plant. A picture of the water side of the eQuest® model is reported in; unfortunately the software does not show both the prime mover and the heat recovery loop.

The first important consideration to make is that eQuest® does not allow the user to recover heat from the *heat recovery loop* to more than one circulation loop. For this reason, the *hot water loop* and the *domestic hot water loop* are considered as one. To better explain: the water heater capacity in the DHW loop is manually set to zero, and the DHW load is, instead, added to the *hot water loop* as a miscellaneous load. This technique has the benefits of simplifying the analysis, without loosing accuracy, but, more importantly, to make it possible for the system

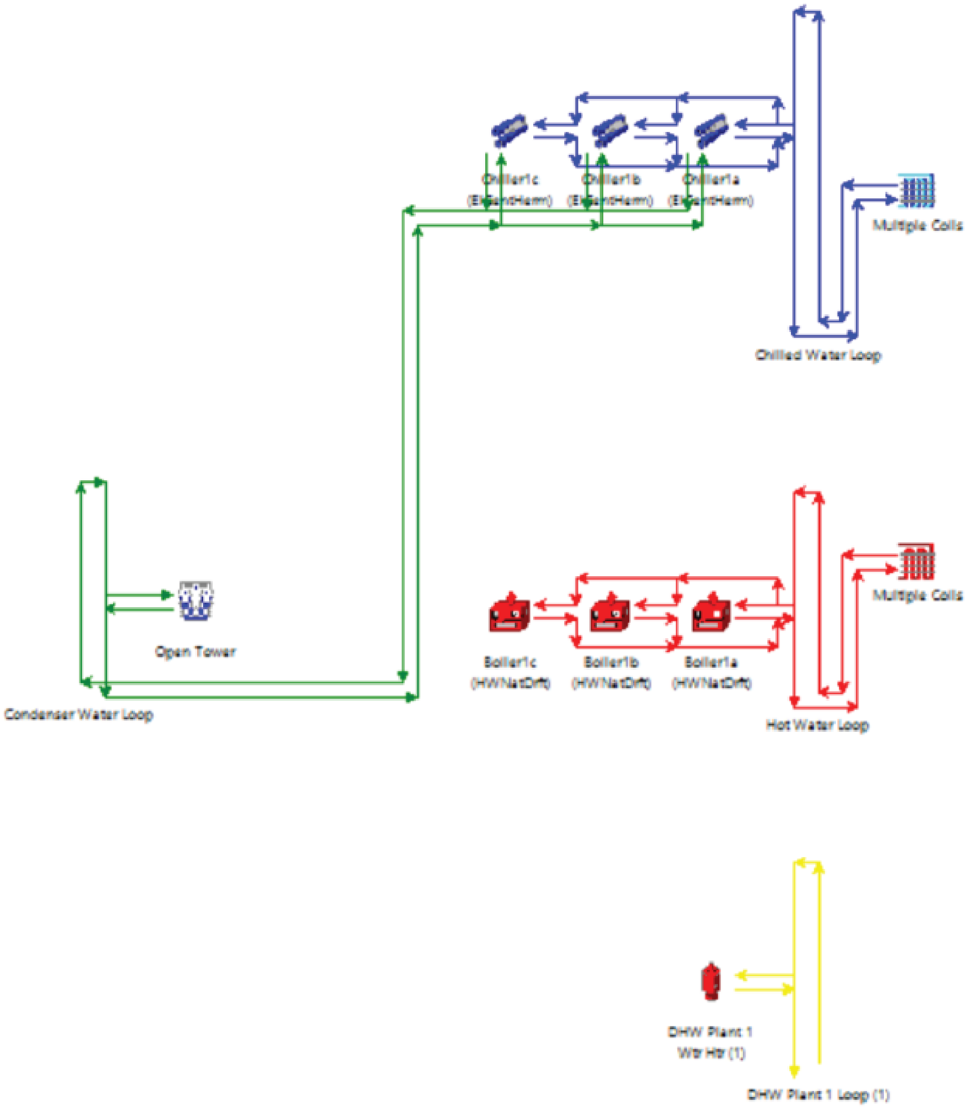

Figure 15: Water side of the system in the eQuest model

to work. In the base model, the *space heating hot water loop* and the *domestic hot water loop* where separate and, their loads where respectively fulfilled by a set of three boilers and a water heater. In the new model, the same loads will be partly satisfied by the *recoverable heat* and, in a second phase, by the TES, strongly reducing the number of hours the boilers run.

The thermal load on the *domestic hot water loop* can be calculated once the water flow rate in the loop and the temperature difference between inlet and outlet are know. The equation used is the following:

$$Q = G \cdot \rho \cdot c \cdot \Delta T \tag{3.2}$$

- Q process load on *domestic hot water loop*
- G process hot water flow rate
- ρ water density
- c water specific heat
- ΔT water temperature difference between inlet and outlet (T_{out}-T_{in})

The temperatures used in the model as T_{in} and T_{out} are 45[F] and 125 [F], respectively. The cooling load of the building, instead, is fulfilled with an electric chiller whose COP is 4.0. The chiller produces the chilled water to feed the *chilled water loop* in order to run the cooling coils in the AHU.

3.5 Electric load analysis

In this section the results obtained by running the simulations on eQuest® are discussed. In this phase the only parameter that varies is the capacity of the turbine that ranges from 500 [kW] to 1300 [kW]. In order to draw some conclusions and make some comments, Figure 16 to Figure 19, show in blue the electric load of the building (before adding the turbine) while, in red, they respectively show the power output of a 500[kW], 700[kW], 1000[kW] and 1300[kW] turbine.

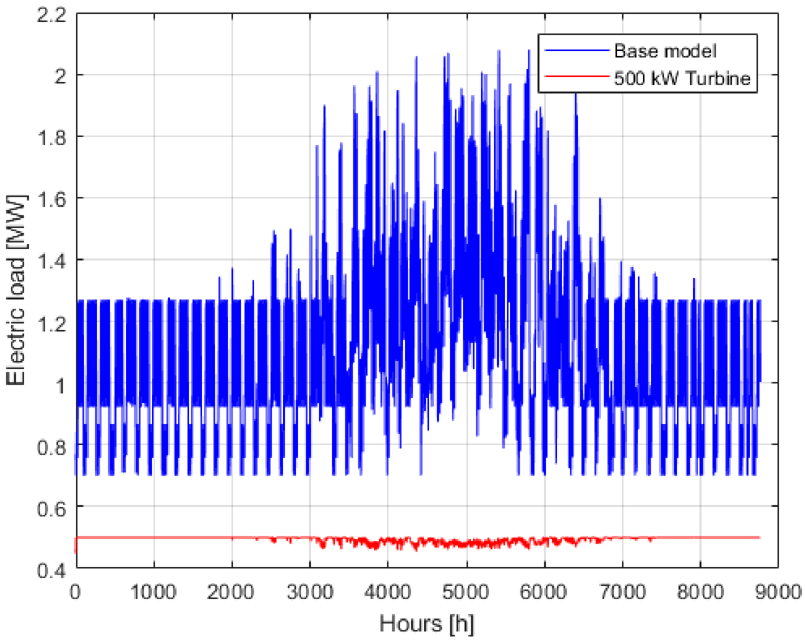

Figure 16: 500 kW turbine electric production

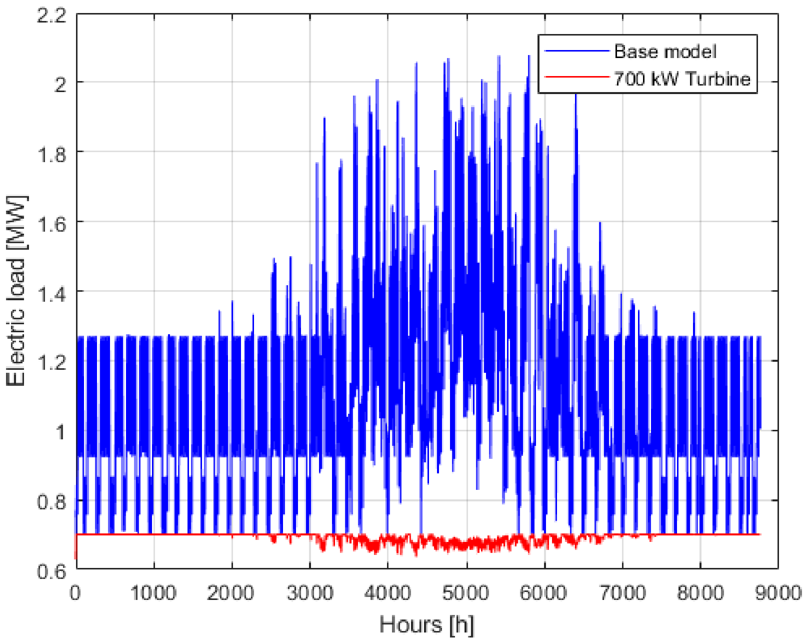

Figure 17: 700 kW turbine electric production

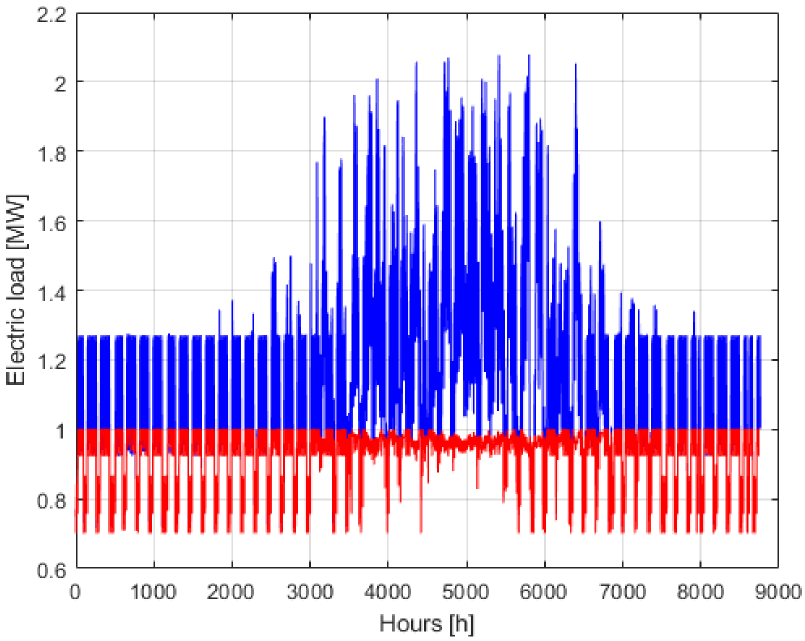

Figure 18: 1000 kW turbine electric production

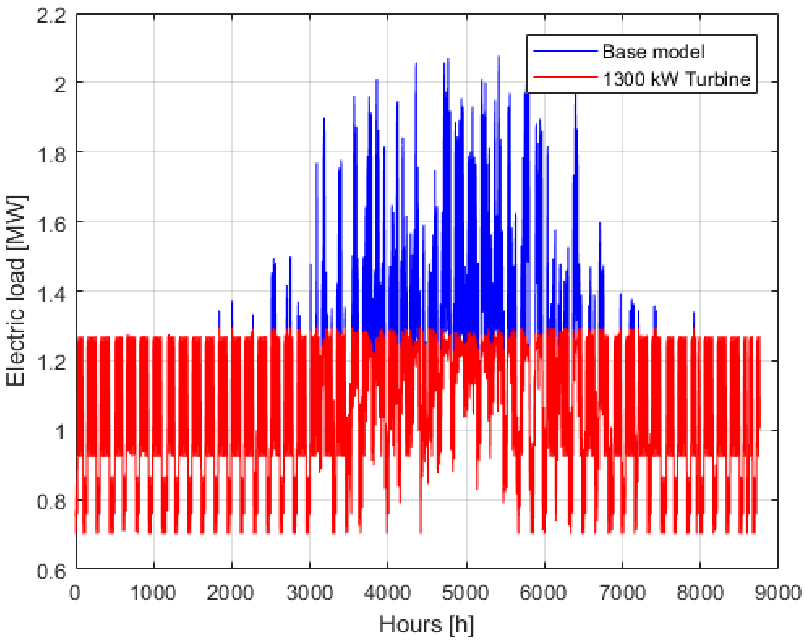

Figure 19: 1300 kW turbine electric production

In these graphs the hour-by-hour difference between the load of the building and the electric production represents the electricity that is purchased from the grid, from here on referred to as *grid electric demand*. Understandingly, the growth in turbine capacity brings to a reduction in the electric demand. On the other hand, a bigger turbine also implies a higher fuel consumption for two reasons. First, a high-capacity machine usually requires more fuel than a small one; at the same time, the bigger the turbine the higher the number of hours it works at partial load.

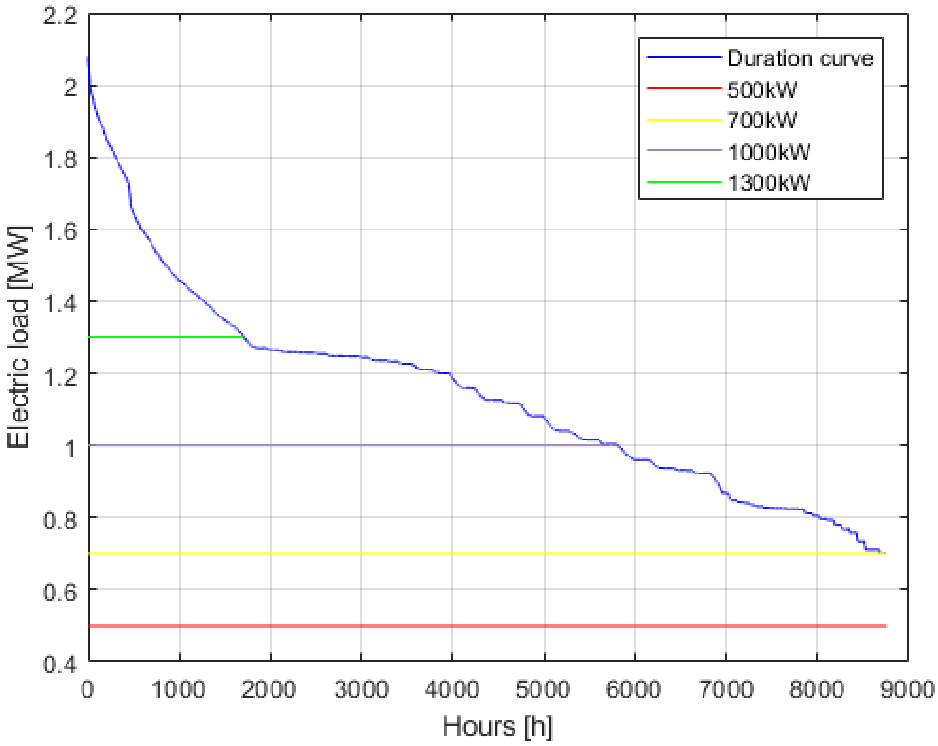

Figure 20: Estimation of the full-load hours for four of the proposed turbine sizes

As anticipated in the previous sections, the partial load operation leads to a reduction in the efficiency of the piece of equipment, meaning that the fuel consumption will be extremely high even when the electric load is low and stable. The *duration curve* is a useful tool to determine the optimal size of the prime mover, as it provides information about the number of hours the desired prime mover should run full load. Once the generator size is chosen, this number is found projecting on the x-axis the intersection between the curve and the capacity of the prime mover. If this one is chosen too close to the origin of the graph, the system will be likely oversized as it will only run full load for a few hours every year and partial load for the remaining hours. In many cases, like gas turbines, working at partial load ratio (PLR) implies a reduction in efficiency. Instead, if the size of the component is reduced, it will operate steadily and at full load for a larger fraction of time, allowing to exploit its best efficiency.

Figure 20 shows the different turbine sizes on the duration curve of the electric load. From this graph the number of full-load hours for each turbine can be extrapolated and becomes thus clear how, for turbines above 1100 [kW], it starts to be inconvenient to install a bigger turbine. The exact numbers representing the fuel consumption and the full-load hours are reported in Table I for further insight.

The other related comment that can be done by looking at Figure 16 to Figure 19 is that the smaller models work steadily throughout the year (because the power output is smaller than the electric load), with slight fluctuations in summer months, unlike the larger ones that are characterized by strong fluctuations even in the heating season. The reason behind the summer fluctuations is due to the influence of the outdoor temperature on the system performances.

TABLE I: **ANNUAL FUEL CONSUMPTION AND FULL-LOAD HOURS**

Turbine size [kW]	Fuel Consumption [MMBtu]	Full-load Hours [h]
500	49,938	8,760
600	59,926	8,760
700	69,914	8,760
800	79,998	8,020
900	90,333	6,889
1000	100,596	5,812
1100	110,757	4,779
1200	120,675	3,964
1300	130,593	1,706

In fact, as demonstrated in Section 2, the external temperature cause a negative effect on the turbine's efficiency. The same issue affects the bigger models as well, however, the simultaneous load variations make it much more hardly detectable. Another possible analysis concerns the reduction in the peak load, when implementing the CHP system. The 500 [kW] turbine is able to provide the power needed to cover the base load of the building, however, it cannot cover any of the peaks, forcing the facility to be dependent from the grid all year long. In this case the peak load goes from 2.08 [MW] to [1.58] [MW]. When using a 1300 [kW] turbine, on the other hand, the facility is grid independent for around 80% of the year and the peak load is reduced from 2.08 [MW] to 0.88 [MW].

3.6 Heat load analysis

The other output of the plant, thus on eQuest®, is the *recoverable heat* available from the turbine. This is provided to the facility as hot water by means of a heat exchanger. By using a spreadsheet containing the heat load of the building and the *recoverable heat*, the actual *recovered heat* can be calculated. Similarly to what was done in the previous section, the heat load and the *recovered heat* for the four representative models are shown in Figure 21 to Figure 24, while the results for the intermediate sizes are summarized in Table II.

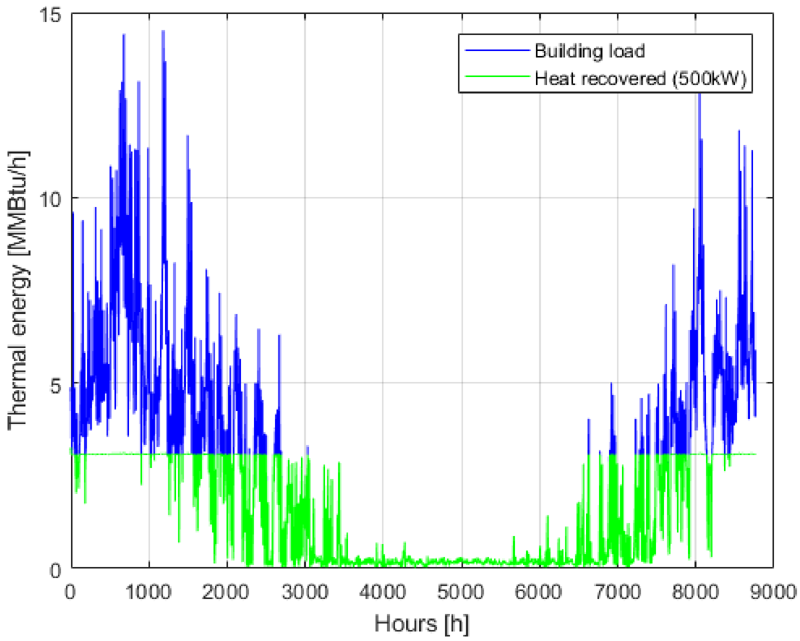

Figure 21: Heat recovered with a 500kW turbine compared to the base model thermal load

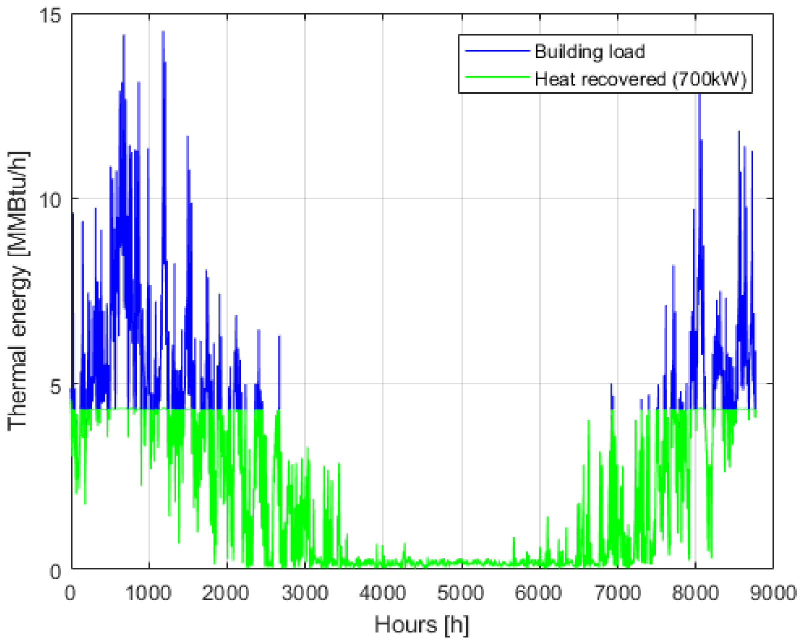

Figure 22: Heat recovered with a 700kW turbine compared to the base model thermal load

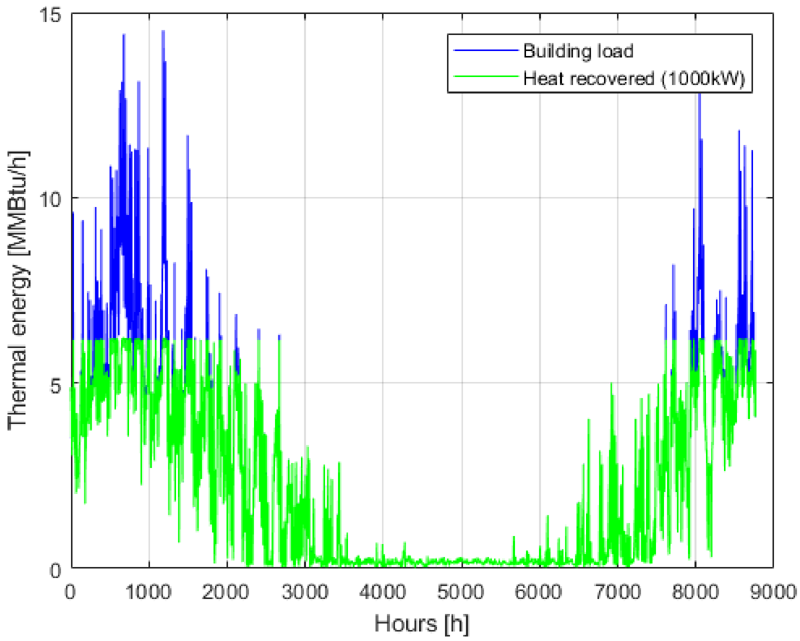

Figure 23: Heat recovered with a 1000kW turbine compared to the base model thermal load

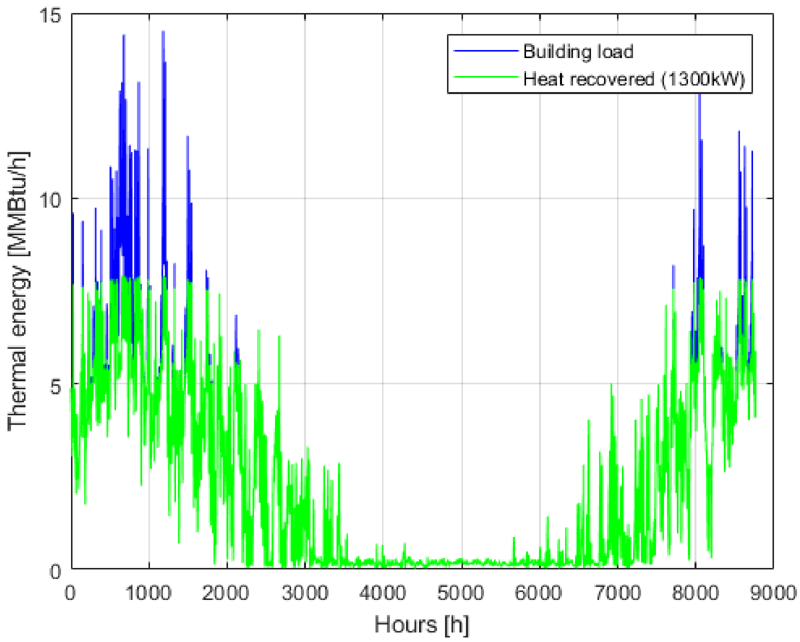

Figure 24: Heat recovered with a 1300kW turbine compared to the base model thermal load

TABLE II: **ANNUAL RECOVERABLE AND RECOVERED HEAT**

Turbine size [kW]	Recoverable heat [MMBtu]	Recovered heat [MMBtu]
500	35,207	16,154
600	42,249	17,644
700	49,290	18,594
800	56,400	19,201
900	63,679	19,544
1000	70,921	19,744
1100	78,084	19,744
1200	85,078	19,850
1300	92,020	19,934

Again, the increase in the turbine size brings with it an increasing reduction in the fuel consumed by the boilers, as the amount of *heat recovered* grows with the GT capacity. It must be specified that, although the boilers are required to work for a smaller number of hours when increasing the turbine size, the overall fuel consumption of the facility grows compared to the base model. At the same time, since the heat available from the turbine follows the electric load (meaning that it raises in the summer when the electric consumption is highest), a larger amount of heat is wasted through the cooling season. The reasons for which part of the *recoverable heat* is wasted are mainly three. One is due the fact that, in some moments of the day, the heat required by the building is lower than that produced by the prime mover. The next possibility is related to the quality of the heat produced: if the thermodynamic characteristics of the *recoverable heat* do not meet those of the hot water in the space heating loop, the heat has to be disposed. The last option, has to deal with the unavoidable irreversibility of the heat exchanger which has an effectiveness of 80%,wasting part of the heat content in the exhaust gases.

The heat recovery has also a strong impact on the heating peak load of the building. In the case of the 500 [kW] turbine, after the heat recovery, the heating peak load goes from 14.5 [MMBtu/hr] to 11.2 [MMBtu/hr]. Instead, when the turbine size is taken to 1300 [kW] the peak load drops to 6.6 [MMBtu/hr]. The total amount of *heat recovered*, on the other hand, grows from 2.4e4 [MMBtu] to 4.5e4 [MMBtu].

3.7 Efficiency analysis

To find the best size for the prime mover some parameters have to be calculated to find the best trade-off between the primary energy consumed, heat recovered, wasted and electricity produced. The *combined heat and power system efficiency* can be defined in many different ways, based on the value given to the different forms of energy. Different definitions of the CHP efficiency have been developed; in this study, only the most one is reported.

3.7.1 The total CHP efficiency

The as-defined calculation method for the efficiency of the system, gives the same importance to the electric and thermal production.

$$\eta_{CHP} = \frac{Q_{rec} + E_{PM}}{F_{PM}} \tag{3.3}$$

- Q_{rec} Actually recovered heat;
- E_{PM} Prime mover electric generation;

- F_{PM} Fuel consumed by the prime mover.

The values of η_{CHP} for all the turbines are reported in Table III

TABLE III: **CHP EFFICIENCY FOR ALL TURBINE MODELS**

Turbine size [kW]	η_{CHP} [%]
500	61.95
600	59.05
700	56.20
800	53.44
900	50.41
1000	47.61
1100	44.93
1200	42.50
1300	39.98

As expected, the smaller the turbine the higher the efficiency. This result is not surprising as low capacity prime movers consume a lower amount of fuel and, at the same time, exploit it better by working at full load for most of the year. The decreasing trend of the CHP efficiency as a function of the GT size is, thus, hardly useful for sizing the generation system. A different parameter is then needed to gain more information. The one used in this study is the *Percentage Reduction in Source Energy Consumption* (PRSEC), discussed in details in the next section.

3.7.2 The Percentage Reduction in Source Energy Consumption

The PRSEC is a parameter that is used to estimate the amount of primary energy saved in the combined generation of heat and power compared to a traditional separated system that produces the same final output. The conventional system is supposed to fulfill the electric load by purchasing all the electricity from the external grid, while the thermal load is satisfied by means of a boiler driven by natural gas. The PRSEC can be expressed and elaborated as follows:

$$PRSEC = \frac{SE_{conv} - SE_{CHP}}{SE_{conv}} \tag{3.4}$$

$$PRSEC = 1 - \frac{SE_{CHP}}{SE_{conv}} \tag{3.5}$$

- SE_{conv} Source Energy consumption for the conventional hospital;
- SE_{CHP} Source Energy consumption for the entire hospital with the CHP system.

These two quantities are calculated by following the ANSI/ ASHRAE Standard 105-2014: Standard Methods of Determining, Expressing and Comparing Building Energy Performance and Greenhouse Gas Emissions [17]. This standard, is meant to provide a comprehensive method for the estimation of the source energy consumption and the correlated greenhouse gases emission. In order to do so, the standard reports the conversion factors accounting for the different forms of energy exploited. For the purpose of this study, since electric and thermal energy are the only forms of energy utilized, the conversion factors needed are:

- 1.09 for the natural gas;

- 3.29 for the electricity.

These factors vary on a geographical base, to take into consideration how the generation and distribution efficiencies change from a region to another one. U.S. is divided in 22 energy market regions and Illinois is part of the eleventh one, the *Reliability First Corporation/ West* (RFCW). The definition of PRSEC presented above not only accounts for the CHP system itself but for all the equipment in the facility that requires a certain amount of energy, e.g chillers and boilers. In fact, SE_{CHP} considers the sum of all the source energy consumption from prime mover but also from the boiler and the electricity purchased. On the other hand, SE_{conv} accounts for the base model consumption, so the source energy consumed by the boiler and to produce the electricity purchased from the grid. A different calculation method for the PRSEC, only accounting for the performances of the on-site generation system will be presented further on in this study. Equation 3.5 and 3.6 can be modified introducing the conversion factors and the energy consumption.

$$PRSEC = 1 - \frac{[SE_{F.B} + SE_{F.PM} + SE_{E.P.}]_{CHP}}{[SE_{F.B} + SE_{E.P}]_{conv}} \tag{3.6}$$

$$PRSEC = 1 - \frac{[F_B \cdot AF_{NG} + F_{PM} \cdot AF_{NG} + E_{purc} \cdot AF_E]_{CHP}}{[F_B \cdot AF_{NG} + E_{purc} \cdot AF_E]_{conv}} \tag{3.7}$$

- $SE_{F.B}$ Source energy consumption related to the boilers fuel consumption;
- $SE_{F.PM}$ Source energy consumption related to the turbine fuel consumption;
- $SE_{E.P.}$ Source energy consumption related to the electricity purchased;

- F_B Fuel consumed by the boilers;
- F_{PM} Fuel consumed by the prime mover;
- E_{purc} Electricity purchased from the external grid;
- AF_E ANSI/ASHRAE conversion factor for electricity;
- AF_{NG} ANSI/ASHRAE conversion factor for natural gas.

To only evaluate the performances of the CHP system, without considering the efficiencies of the rest of the equipment (like boilers and chillers), another index, here referred to as *on-site PRSEC* can be calculated as follows.

$$PRSEC_{OS} = 1 - \frac{[SE_{F_{PM}} + SE_{E.P.}]_{CHP}}{[SE_{Q_{rec}} + SE_{E_{PM}}]_{conv}} \tag{3.8}$$

$$PRSEC_{OS} = 1 - \frac{[F_{PM} \cdot AF_{NG}]_{CHP}}{[F_B \cdot AF_{NG} + E_{PM} \cdot AF_E]_{conv}} \tag{3.9}$$

$$PRSEC_{OS} = 1 - \frac{[F_{PM} \cdot AF_{NG}]_{CHP}}{[\frac{Q_{rec}}{\eta_B} \cdot AF_{NG} + E_{PM} \cdot AF_E]_{conv}} \tag{3.10}$$

- $SE_{F_{PM}}$ Source energy consumption related to the turbine fuel consumption;
- $SE_{Q_{rec}}$ Source energy consumption related to the fuel consumption to replace Q_{rec};
- $SE_{E_{PM}}$ Source energy consumption related to the electricity produced by the GT
- F_B Fuel consumed by the boilers to replace the heat recovered;
- F_{PM} Fuel consumed by the prime mover;
- Q_{rec} Recovered heat from the CHP system;

- E_{PM} Electricity purchased from the external grid;
- η_B Efficiency of the boilers;
- AF_E ANSI/ASHRAE conversion factor for electricity;
- AF_{NG} ANSI/ASHRAE conversion factor for natural gas.

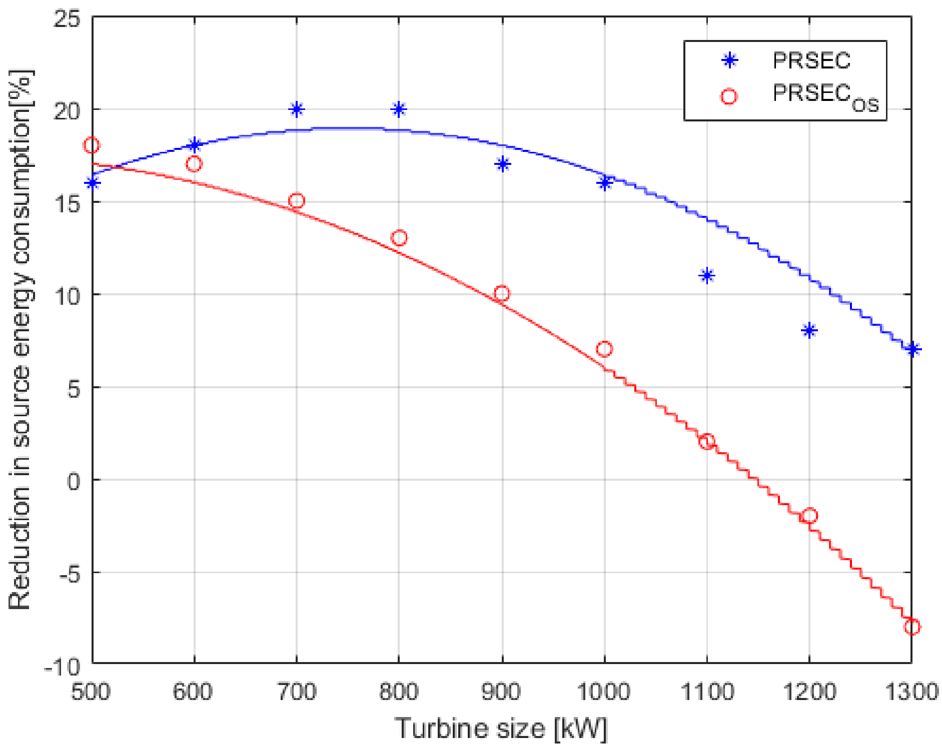

Figure 25: PRSEC and on-site PRSEC as a function of the turbine size

The results obtained from both approaches are reported in Figure 25. From an analysis of this graph, it can be concluded that, according to the *PRSEC* the optimal prime mover would have a capacity of 800 [kW]. On the other hand, the second approach shows that a 500 [kW] turbine has better performances compared to the others. Some comments can be made to get to an univocal conclusion. The on-site PRSEC approach has as an optimal result a smaller turbine because of a better exploitation of the *recoverable heat*. In fact, producing a smaller amount of heat, also reduces the amount of *wasted recoverable heat*, leading to a more efficient system. However, when looking at the problem from a wider perspective (i.e. looking at PRSEC), a larger prime mover is definitely more convenient as it enables a better coverage of the electric load, reducing the more expensive need of purchasing the electricity from the grid. So, since it can be concluded that the on-site PRSEC only provides a partial description of the system, it will not be used in the rest of the study.

CHAPTER 4

THE THERMAL ENERGY STORAGE

A *Thermal Energy Storage* (TES) is a device designed to store energy at either high or low temperature with the goal of allowing to decouple the moment of the thermal energy generation from that of its utilization. Usually, TES consists in a highly insulated tank filled with a material, referred to as *heat storage medium* (HSM). The technical solutions to store the energy are several; the most used are either based on sensible or latent heat. In the first case, the thermal energy is stored by inducing a temperature increase in the HSM, while in the latter, a changing in phase of the HSM is exploited. Other possibilities exist, like thermochemical storage, but are still in a R&D phase and are not treated in this work. In fact, the kind of storage chosen for this study is a high-temperature water, sensible thermal storage.

The most important advantage provided by a TES is that it enables storing part of the *recoverable heat* when it exceeds the thermal load, that would otherwise be wasted. At the same time, when the *recovered heat* is not enough to meet the build needs, the storage could fulfill part of the load, preventing the boilers from running. Hence, the implementation of a hot TES coupled with a CHP, allows to further improve the exploitation of the source energy. Other benefits given by TESs are listed below:

- **Enhancement of the facility safety:** the presence of a water energy storage can be integrated with the fire protection system, serving as a reservoir for emergency cases;

- **Improvement of the system reliability:** the energy storage allows to satisfy part of the load in the unfortunate case of an interruption in the natural gas supply;
- **Reduction in GHG emission:** by preventing boilers operation, the amount of fuel burned is decreased and, as a consequence, the emission of the pollutants related with the combustion;
- **Improvement of the generation capacity:** as anticipated, especially in a FEL CHP system, part of the heat that would have gone wasted in case of a demand mismatch, can be saved and used later;
- **Shifting the energy purchases to more convenient periods:** if the facility energy rates are time-based, it can be useful to buy and store the energy when the rates are low and use it when the prices grow.

Most of the actual thermal storage exploit the phenomenon of *stratification*. Thermal stratification is caused by the temperature difference, thus a variation in the fluid density, occurring between the inlet and outlet water. A stratified TES is usually divided into two thermal zone, a cold and hot one, with a thermal gradient in between, called *thermocline*[18]. The cold water lays on the bottom of the tank, while the hot water floats in the upper part. This approach, tends to improve the efficiency of the TES by reducing or completely avoiding the mixing of the fluid between the two thermal zones[18]. However, eQuest® does not support the dynamics of a stratified tank. The storage here analyzed is, hence, simplified and considered as *fully mixed*, meaning that the fluid temperature is uniform.

4.1 Working principle

In this section the principle on which the thermal storage is based, is explained. As anticipated, the model here implemented is a *fully mixed thermal energy storage*, whose mathematical description is far more simple compared to the more realistic stratified tank.

Every substance, in this case liquid water, has an energy content proportional to its temperance. The hotter the substance, the higher its energy (and the quality of its energy) will be. This principle can be formulated as follows:

$$E = m \cdot c \cdot (T_2 - T_1) = \rho \cdot c \cdot V \cdot (T_2 - T_1) \tag{4.1}$$

- E Thermal energy needed to raise the temperature of an amount m of water from T_1 to T_2;
- m Mass of the material to heat;
- c Specific heat of the substance;
- ρ Density of the substance;
- V Volume of the substance;
- T_1 Initial temperature of the substance;
- T_2 Final temperature of the substance.

Equation 4.1 is valid for the heat transfer method referred to as *sensible* that is thus based on a rise or reduction in the temperature of the object. As anticipated, the quality of the energy is extremely relevant when designing the system; this is basically dependent on the amount of water heated and on the ΔT it undergoes. As an example, a unit of thermal energy (1 [kWh]) can be stored by heating to 33.5[F] 1.1[US tons] of water, however this heat will be hardly exploitable for purposes like space heating. However, the same amount of energy can be also stored by heating up to 189 [F], just 22 [lb] of water. High-temperature heat is much more useful and easily exploitable for the applications treated in this study and many others.

The working principle of any type of storage, can be schematized in three phases: charge, storage and discharge. In particular, for a thermal energy storage, these three phases are explained as follows:

- **Charge:** the heat (from the exhaust gases in this specific case) is transferred in a heat exchanger to the TES;
- **Storage:** the heat is mostly kept inside the tank, although a certain percentage is lost through the insulation towards the environment (for a hot TES);
- **Discharge:** through another heat exchanger, the heat in transferred to the user (in this case the hot water coils in the space heating loop).

4.2 Technical evaluation and integration with the CHP system

Some aspects need to be assessed, when introducing a TES in a facility, in order to ensure a proper functioning for the facility's necessities. The first thing to decide would be the capacity, hence the size, of the tank. This process will be widely discussed in a separate section. Then, the material and the storage strategy have to be determined. As anticipated, the material chosen is water, while the storage strategy is based on sensible heat. The reasons behind the choice of water are due its high specific heat, compared to many other materials, low cost and availability. The high specific heat (c=1.004 [Btu/lb_mF]) allows the system to work easily in a temperature range like the one required by space heating applications, avoiding the need of pressurizing the water. Rocky and ceramic materials, instead, usually have much lower values of specif heat but, their high density makes them suitable for operations in a wider temperature range. Once the storage method, the heat storage material and the charge and discharge loops are chosen, the operating temperatures of the storage can be evaluated. The loop chosen to charge the TES is the *heat recovery loop*, where the exhaust gases are assumed to have a temperature between 850 [F] and 950 [F]. The discharge loop, instead, is the *space heating hot water loop*, whose working temperature on eQuest® had been set to 170 [F]. Considering a minimum temperature difference of 30 [F] between the discharge loop and the water inside the tank, the maximum operating temperature of the storage is set to 200 [F]. Since the tank is not pressurized, a higher temperature would cause an undesired phase change in the water. On the other hand, the minimum temperature cannot be lower than the one of the *space heating loop*, so it is set equal to 170 [F].

4.2.1 Evaluation of the tanks

Once the working temperatures and the *heat storage medium* have been decided, the only parameter that can be modified to vary the capacity of the storage tank is its volume. One of the main goals of this study is to evaluate the impact of a high-temperature energy storage on a large health care facility energy consumption. To do that, the capacity of the tank is varied in a wide range from 2 [MMBtu] to 14 [MMBtu], so that it is possible to determine whether a large TES produces a comparatively much higher *source energy consumption* than a smaller one. Since the capacity range is known, the volume range can be determined as a consequence, so that more specific models from actual manufacturers can be chosen to proceed with the analysis. The minimum and maximum volumes associated with the capacities above are, considering a water density of 8.078 $[lb_m/gal]$ and a specific heat of $1.004[Btu/lb_mF]$, respectively 8,220 $[gal]$ and 57,540 $[gal]$. For this study, Highland Tank® is the manufacturer designated for the choice of the tanks. Their products are compliant with many standards[19]; in particular their HighDRO® line meets the following standards:

- ASME Code, Section VIII, Division I
- American Water Works Association AWWA D100 - "Standard for Welded Steel";
- National Fire Protection Association NFPA Standard No. 22, "Water Tanks for Private Fire Protection";
- National Sanitation Foundation (NSF)

The models are chosen from their catalog among the "HighDRO® Vertical Tanks"; the commercial sizes, as expected, are not exactly coincident with the ones calculated above. Hence, the tanks adopted from now on will be in the range of 8,000 $[gal]$ and 57,500 $[gal]$. The correspondent capacities are 1.95 [MMBtu] and 13.99 [MMBtu].

The tanks used for this study are also eligible for credits in the LEED Certification process, in case LEED is meant to be pursued.

4.2.2 Thermal losses evaluation

The last aspect that needs to to be assessed before actually modeling the TES, concerns the *heat losses* through the tank. As the tanks are not ideal objects, it is impossible to avoid losing part of the heat stored towards the environment. In this section the heat transfer methods that cause *heat losses* to occur are explained (it must be anticipated that radiation is considered in this analysis). Furthermore, a calculation method for the estimation of the *heat loss coefficient* is addressed.

The first mechanism the causes *heat loss* is *conduction* that consists in a transfer of heat due to a temperature gradient in a solid. In this case the transfer occurs without any bulk movement of the matter. An example can be a wall whose faces are characterized by two different temperatures: a heat flux will occur from the hot to the cold side, so that part of the heat content on the hot side is dispersed towards the cold one (or gained by it). The conductive mechanism is described by the *Fourier's law of conduction*; in the case of a tank with a fully-mixed fluid inside, the one-dimension form of the law can be used, as both the temperatures of the inner and outer side of the tank can be considered uniform. Conduction is only a function of the material, its geometry and temperature difference:

$$\dot{q} = -k\frac{dT}{dx} \tag{4.2}$$

For a plane wall the equation can be modified as follows:

$$\dot{q} = \frac{\dot{Q}}{A} \rightarrow \dot{Q} = -kA\frac{dT}{dx} = kA\frac{T_{high} - T_{low}}{L} \tag{4.3}$$

- $\dot{q}$ Heat flux through the solid $[\frac{Btu/h}{ft^2}]$;
- $\dot{Q}$ Heat transferred through the solid $[Btu/h]$;
- k Thermal conductivity of the material $[\frac{Btu/h}{ftF}]$;
- A Cross section of the solid $[ft^2]$;
- L Thickness of the solid $[ft]$;
- $T_{high} - T_{low}$ Temperature difference between across L $[F]$.

For a cylindrical geometry, instead, Equation 4.2 is manipulated to reach the following form:

$$\dot{Q} = \frac{2\pi Lk(T_{high} - T_{low})}{ln(r_2/r_1)} \tag{4.4}$$

- L Length of the cylinder (in this case is the height of the tank);
- r_2 Cylinder outer radius;
- r_1 Cylinder inner radius;

The second mechanism causing the heat to be transferred to the outside is *convection*. Unlike *conduction*, *convection* occurs when a there's a temperature difference between a solid and a moving fluid. In this specific case the surface is the outer side of the tank and the fluid is the outdoor air. The convective mechanism can have different causes and is, hence, accordingly classified.

- **Forced convection:** occurs if an external force causes the fluid to move (e.g. wind or pumps);

- **Free or natural convection:** it is caused by the buoyancy forces caused by the density difference due to a temperature gradient in the fluid.

A schematic representation of the convective mechanism is provided in Figure 26 for a clearer explanation of the phenomenon.

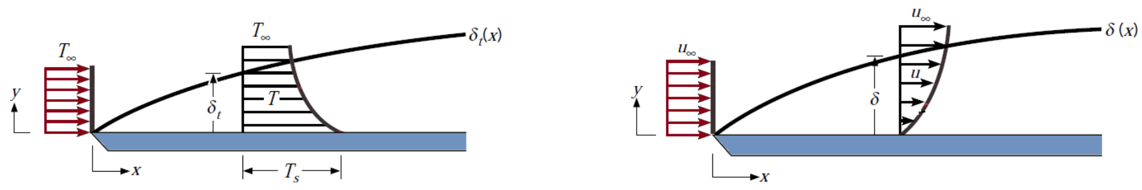

Figure 26: Convective Heat Transfer Temperature and Velocity profiles

A boundary layer where the velocity of the fluid is proximate to zero and most of the temperature gradient occurs, has a thickness δ. Outside this layer, the temperature is considered to remain constant ($T = T_\infty$). The heat flux describing this process is written as follows:

$$\dot{q} = \frac{\dot{Q}}{A} \rightarrow \dot{Q} = \frac{k(T_w - T_\infty)}{\delta} \tag{4.5}$$

Where all the symbols have the same meaning as in the previous equations except:

- δ Thickness of the boundary layer;

- $(T_w - T_\infty)$ Difference between the temperature of the external wall of the tank and the undisturbed temperature of the fluid.

The thickness δ is a function of several parameter: first, the kind of flow, laminar or turbulent, estimated through the Reynolds number, the pressure gradient, the geometry of the wall (its surface area) and the Mach number. To simplify the analysis the *heat transfer coefficient* is introduced as the ratio between k and δ and empirically calculated, using the correlation for forced convection in an air flow.

$$h = 10.45 - v + 10\sqrt{v} \tag{4.6}$$

To be more precise the *heat transfer coefficient* should be calculated by first calculating the Nusselt and Raynolds numbers, however, for the purposes of this study, the correlation above provided a sufficient degree of approximation. In Equation 4.5, v is the relative speed between the wall surface and the air in [m/s].

Once a method for the calculation of the *heat transfer coefficient* has been established, the *heat losses* can be calculated through the *Newton's cooling law*:

$$\dot{Q} = hA(T_w - T_\infty) \tag{4.7}$$

To determine the *heat loss coefficient*, two more assumptions are made:

- The tank is located outdoors to avoid possible space constraints;

- The tank has a cylindrical shape and is positioned vertically, with its lower surface touching the ground.

The last assumption gives the chance to neglect the heat losses towards the ground, so just the lateral surface and the top of the tank are considered to be dissipating heat.

In order to determine an expression for the *heat loss coefficient* the overall *thermal resistance* needs to be calculated. Some of the data needed to do so concern the structure of the tank, especially the thickness and the thermal conductivity of the metallic and insulation layer. For high-temperature energy storage, Highland Tank® has two insulation options[19]:

- Spray-on polyurethane foam with acrylic sealer ($k_{ins} = 0.0104[\frac{Btu/h}{ftF}]$)
- External fiberglass batt with metal jacketing ($k_{ins} = 0.0208[\frac{Btu/h}{ftF}]$)

For this study the polyurethane foam was chosen as the tank insulation material. The tank itself, instead, is manufactured with 100% recyclable Stainless Steel from 304, 304L, 316 or 316L stainless steel to prevent the tank from corrosion ($k_{steel} = 8.32[\frac{Btu/h}{ftF}]$) [19].

The temperature of the inner side of the tank is assumed to be at the same temperature of the water (that can vary from 170[F] to 300[F]), here referred to as T_1. T_2 and T_3 are, respectively, the temperatures of the inter-space between the steel and the insulation and, the temperature of the outer side of the tank. Finally, T_{amb} is the outdoor temperature at a distance δ from the tank; L_1 and L_2 are the thicknesses of the steel and insulation layers.

The three equations that describe the heat flux through the top of the tank, that is considered as a plane wall, and towards the environment are, thus, reported below:

$$\frac{\dot{Q}}{A} = k_{steel} \cdot \frac{T_1 - T_2}{L_1} \tag{4.8}$$

$$\frac{\dot{Q}}{A} = k_{ins} \cdot \frac{T_2 - T_3}{L_2} \tag{4.9}$$

$$\frac{\dot{Q}}{A} = h \cdot (T_3 - T_{amb}) \tag{4.10}$$

Overall, the heat transfer process through this part of the tank can be rewritten in the more compact form:

$$\dot{Q} = \frac{T_1 - T_{amb}}{R} \tag{4.11}$$

Where R is the total equivalent resistance, that is described as follows:

$$R = \frac{L_1}{Ak_{steel}} + \frac{L_2}{Ak_{ins}} + \frac{1}{hA} \tag{4.12}$$

The same procedure can be repeated for the cylindrical part of the tank, properly modifying the equations for this geometry.

$$\dot{Q} = \frac{2\pi Lk_{steel}(T_1 - T_2)}{ln(r_2/r_1)} \tag{4.13}$$

$$\dot{Q} = \frac{2\pi Lk_{ins}(T_2 - T_3)}{ln(r_3/r_2)} \tag{4.14}$$

$$\dot{Q} = 2\pi r_3 Lh(T_3 - T_{amb}) \tag{4.15}$$

Once again, the overall thermal resistance is:

$$R = \frac{ln(r_2/r_1)}{2\pi k_{steel}L} + \frac{ln(r_3/r_2)}{2\pi k_{ins}L} + \frac{1}{2\pi r_3 Lh} \tag{4.16}$$

4.3 The Thermal Energy Storage model

The initial intent of this study was to introduce the model of a TES in the eQuest® model of the hospital. As a matter of fact, this has been done, however the results obtained were unrealistic and did not reflect the actual operations of the system for the following reasons:

- Despite the *heat recovery loop* had been selected as the charge loop, it was found that the TES was actually charged using the boilers;
- Once charged, the storage did not release its thermal content to the *space heating hot water loop*, thus it did non discharge.

This results, led to the conclusion that eQuest® has some inner strong limitations as far as concerns the integration between a hot thermal storage and a cogeneration system. Such limitations are mainly related to the control of the different pieces of equipment. Once the poor reliability of the eQuest® results was proved, a different method to model the TES was implemented. The tool used for the following modeling is an Excel spreadsheet, were the hour-by-hour data concerning the building loads, the gas turbine and boilers production and consumption were retrieved from the CHP model on eQuest®. The amount of energy that could be stored in TES and then discharged, was modeled considering the amount of *recoverable heat* from the prime mover, the heat load of the facility and the thermal losses (calculated as shown in the previous section). A different spreadsheet was created for every turbine size, with the possibility of changing the capacity of the storage and determine how the profiles of the *total heat recovered* changed. This tool was also used to calculate the parameters needed to optimize both the turbine and the storage size. The sizing process is explained in details in the next section.

4.4 The sizing process

In order to properly size the system, both the prime mover and the TES capacities have to be determined to find the optimal combination that leads to the highest reduction in source energy consumption. Since two variables need to be determined, a multi-variable, iterative, optimization process is implemented. The *objective function* chosen for this analysis is the PRSEC, whose calculation method was illustrated in Section 3.7.3. In this case, however, the value of the boilers fuel consumption is calculated again to account for the higher amount of heat recovered through the storage system. In order to do so, it is necessary to evaluate the amount of fuel saved by using the storage instead of the boilers. This quantity was calculated in Excel as an *Equivalent Fuel Content* (EFC), evaluating the amount of fuel that a boiler (with the same characteristics of the one installed) would consume to produce the same thermal energy stored in the tank.

$$EFC = \frac{Q_{stored}}{\eta_{boiler}} \tag{4.17}$$

The optimization process is performed by first setting the volume, thus the capacity, of the storage and varying the turbine size. Once a first optimal size for the prime mover is found, this is frozen while the capacity of the TES is varied in the range established earlier in the study.

The process is alternatively repeated as many times as needed, until two similar enough results are obtained in two subsequent steps, in term of difference in the in the objective function.

4.4.1 First iteration

In the first step of the process, the turbine size ranges from 500 [kW] to 1300 [kW], while the storage volume is set to 20,000 [gal]. Table IV shows the complete results from this first step. The turbine that leads to the best PRSEC, is the 800 [kW] one, with a total PRSEC of 23.94%, that is quite a notable result compared to the base model that is 19.86%.

TABLE IV: **FIRST ITERATION: PRSEC VALUES VS TURBINE SIZE WITH A TANK CAPACITY OF 20,000 GAL**

Turbine size [kW]	**PRSEC** [%]	η_{CHP} [%]
500	20.23	62.30
600	22.15	59.30
700	23.31	56.38
800	23.93	53.55
900	21.84	50.49
1000	19.25	47.67
1100	16.00	44.97
1200	12.46	42.52
1300	7.57	39.98

4.4.2 Second iteration

In the second step, the turbine is the one obtained from the previous iteration and the storage varies from 0 [gal] to 57,500 [gal]. This time, it can be noticed (Figure 27) that the

PRSEC has an increasing trend, so it is not possible to find an optimal value. In fact, the PRSEC grows from 19.9% to 24.03% and, if ideally increasing the storage capacity the PRSEC hardly goes beyond 24%. A graphic representation of the trend is provided in Figure 27.

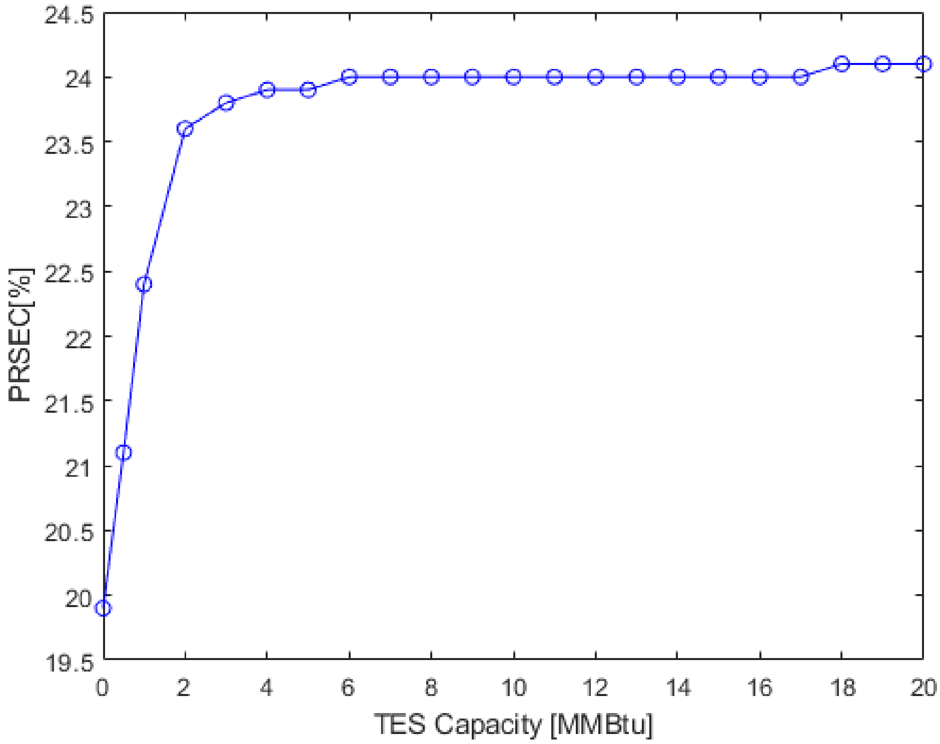

Figure 27: Second iteration: PRSEC values vs TES capacity with a turbine size of 800 kW

It is intuitive that the larger the storage the larger the amount of recovered heat. However, a large increase in storage capacity does not always lead to an equally substantial improvement in the system performances. An explanation for that could rely in the winter consistency of the heating load of the building, that, due to the short term capacity of the storage, might result in a small influence on the consumption. The trend line in Figure 27 shows that the PRSEC is stable at around 24%, for TES capacities above 5 [MMBtu], that correspond to a storage volume of 20,000[gal].

Since a reference dimension for the TES still has to be picked, other criteria are taken into account for this choice. An important driver in this kind of analysis, is related to costs. An economic analysis should account for the following elements, in order to determine if the savings produced justify the expense.

- Investment cost;
- Labor cost (e.g. installation): this is influenced by the material and the type of the tank (steel tanks tend to be more expensive than aluminum tanks to install, just like double-wall tanks compared to single-wall ones)
- Operation and Maintenance (O&M) cost;
- Financial incentives;
- Daily peak loads;
- Cost of fuel;

A detailed economic evaluation is not the purpose of this study because of the fickle nature of the above-mentioned costs, their strong dependence on the kind of contracts the customer is subjected to and the characteristics of the facility. However, some guide lines are here provided to enable a reasonable choice of the equipment. Both the investment and installation costs grow exponentially with the size of the tank. In fact, although the manufacturer does not provide a price list for its products, it is possible to retrieve the average costs for similar tanks online [20]. For big tanks (above 5,000 [gal]) the price tends to double for every 5,000 [gal] increase in volume. Considering that, the most reasonable choice seems to be the smallest tank, among those proposed by Highland Tanks®, that enables to reach the 23% PRSEC. This would be a 20,700 [gal] tank, able to store up to 5 [MMBtu].

4.4.3 Third iteration

The last step of the process consists in repeating the calculation for the PRSEC using the 5 [MMBtu] storage and varying again the turbine size. The results are reported inTable V. The 800 [kW] turbine is again the best option with a PRSEC of 23.94%. So the the final configuration for the cogeneration plant is provided with a 800 [kW] gas turbine and high-temperature energy storage of at least 20,000[gal]. The final results showing the hour-by-hour profile of the heat recovered is shown in Figure 28.

TABLE V: **THIRD ITERATION: PRSEC VALUES VS TURBINE SIZE WITH A TANK CAPACITY OF 20,700 GAL**

Turbine size [kW]	**PRSEC** [%]	η_{CHP} [%]
500	20.25	62.31
600	22.16	59.31
700	23.31	56.38
800	23.94	53.56
900	21.84	50.50
1000	19.26	47.67
1100	16.02	44.97
1200	12.47	42.52
1300	7.57	39.98

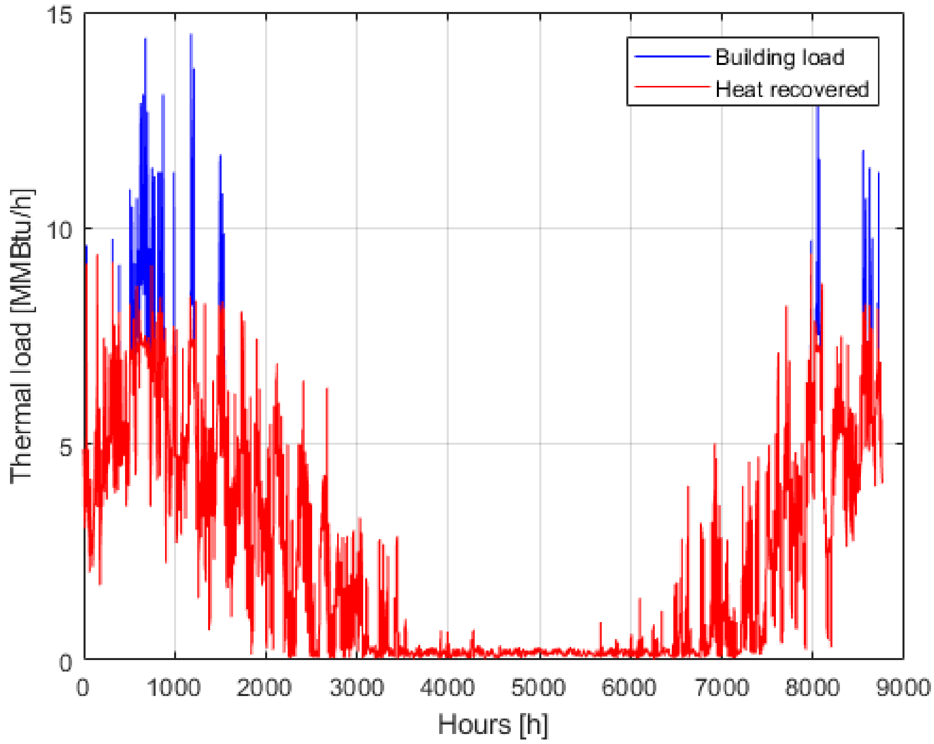

Figure 28: Heat recovered from the CHP system and the TES

CHAPTER 5

THE COMBINED COOLING, HEAT AND POWER PLANT

This chapter is meant to provide an overview of the chiller technology, especially with the goal of implementing an absorption chiller in the CHP system, to obtain a *combined cooling, heat and power system*. In fact, as it will be further explained, absorption chillers can exploit the *recoverable heat* to produce the chilled water used to run the cooling coils of the air handling unit. The objective is, thus, to determine the effect that the implementation of this kind of technology has on the performances of system, in terms of absolute consumption but mostly of percentage reduction in source energy consumption. In order to do that, the different types of chiller are investigated in terms of working principle and performances; an eQuest® model is then proposed based on previous studies[12] and, finally, a sizing process is performed to obtain the optimal sizes of all the pieces of equipment.

A *combined cooling, heating and power system* exploits one single energy source (in this case natural gas) to obtain three products: electric and thermal energy, like in a cogeneration system, but also cold water. For this reason, this kind of systems are also referred to as *trigeneration systems*. Their biggest advantage is the possibility of covering, even if just partially, all the energy needs of a building using a single a system. Trigeneration plants usually show overall efficiency in the order of 85%, extremely higher than the average 40% efficiency typical of traditional separated production plants[21].

5.1 The chiller technology

A device whose function is to remove a certain amount of thermal energy from a system and transfer it to another one that is at a higher temperature, is referred to as a *chiller*. In order to achieve this goal, without violating the *second principle of thermodynamics*, chillers can use different forms of energy that allow to complete an inverse thermodynamic cycle. Based on that, the type of chillers here discussed can be classified as *vapor compression* and *absorption* chillers.

5.1.1 Vapor compression chillers

Vapor compression chillers represent the most common technology for many applications like medium size HVAC systems, food industry and chemical processes. Their operation is based on a thermodynamic cycle that can be approximated with an inverse Rankine cycle, called Clausius-Rankine cycle [22]. The transformations and the key components of the of a *vapor compression chiller* are represented in Figure 29 and Figure 30.

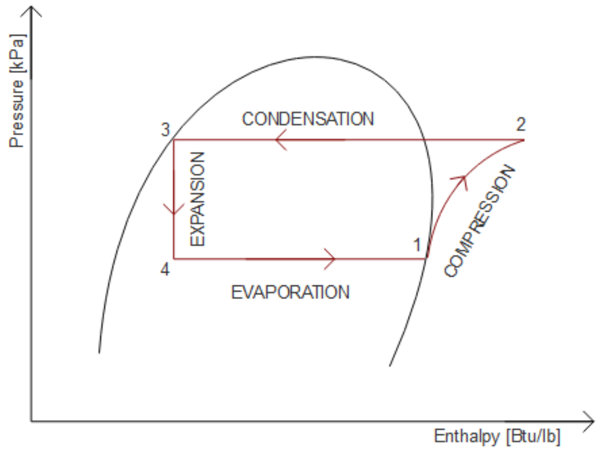

Figure 29: Thermodynamic transformations of a refrigeration cycle

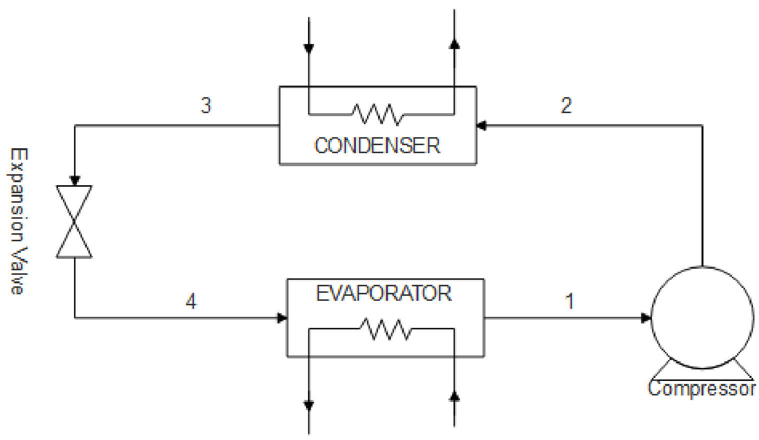

Figure 30: Schematic representation of the chiller components

The four key components that allow a chiller to work properly are the following:

- Compressor;
- Condenser;
- Expansion valve;
- Evaporator.

The refrigerant, that is in the state of *saturated vapor*, is compressed by the compressor after exiting the *evaporator* and reaches the state of *overheated vapor*. This vapor has higher temperature compared to the environment, so it releases part of its thermal energy to it by condensing in heat exchanger that is hence referred to as *condenser*. After the condensation process is completed, the refrigerant is in the state of *saturated liquid* and is ready to undergo an expansion in the *lamination valve*. The lamination causes a strong reduction in both the pressure and the temperature of the fluid, that is finally entering another heat exchanger, the *evaporator*. Here, thanks to the temperature and pressure, that are lower with respect to the external environment, the refrigerant subtracts heat from the environment, cooling it down. In doing that, it undergoes an evaporation process that takes it back to the starting point of the cycle.

The performances of this kind of equipment are usually estimated through the calculation of a parameter called *Coefficient of Performance* (COP). The COP measures how well the chiller is able to convert the input work into a useful effect, which the cooling of a certain environment. The COP is defined as follows:

$$COP = \frac{Q_-}{W} \tag{5.1}$$

- Q_- Thermal energy removed from the environment;
- W Work performed on the cycle.

COP is influenced by many factors, among which the evaporating and condensing temperature, the fluid used as a refrigerant and, obviously, the different pieces of equipment are the most important. The control system and a proper maintenance, however, have also a strong effect on the actual performance of the system.

5.1.2 Absorption chillers

An *absorption chiller* is different from a *vapor compression* one because it exploits a thermochemical process to cause the refrigerant evaporation and condensation, thus using a high-temperature source instead of an electric compressor. This is done by using two fluids: a *refrigerant* (e.g. water) and an absorbent (e.g. LiBr)[7]. In order to enable this process, it is of critical importance that the two fluids show a strong chemical affinity, meaning that one of the two has to be able to easily dissolve in the other one. This property is highly influenced by the relative concentrations of the two fluids in the mix[7]. Two of the most common mixtures are the following:

- $NH_3 - H_2O$: ammonia is used as a refrigerant while water is the absorbent;
- $H_2O - LiBr$: the refrigerant is represented by water, while Lithium Bromide is the absorbent.

For the following considerations, the $H_2O - LiBr$ mixture will be considered. The principles on which an absorption chiller relies can be summarized as:

- Water at extremely low pressure and low temperature (40[F]) can easily evaporate. These are the conditions that can be found in an absorption chamber (840 [Pa]);
- The $H_2O - LiBr$ mixture can be distilled, meaning that, applying a certain amount of heat, the water evaporates while the salt (LiBr) stays in the bottom of the chamber. The two substances are hence separated;
- The liquid salt LiBr, has the ability of attracting the water vapor molecules. So, as anticipated, the higher the relative amount of water, the worse is the absorption capacity of the salt.

For this kind of equipment, the key components are the following;

- **Generator:** it is linked to the high-temperature source (in a CCHP system this would be the hear recovery loop;
- **Condenser:** it is linked to another heat reservoir, but with a lower temperature (e.g. a cooling tower or the outdoor environment);
- **Evaporator:** it is the component linked to coldest source, which is the one that has to cooled down (e.g. the water of the *chilled water loop*);
- **Absorber:** it is connected to cold heat source and is used to restore the proportions of refrigerant and absorbent in the mixture.
- **Pump and lamination valve**

A graphic representation of the system is provided in Figure 31

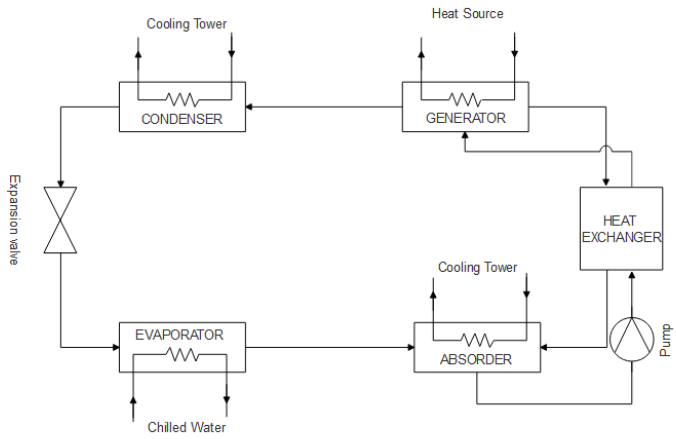

Figure 31: Schematic representation of an absorption chiller

Starting the cycle from the generator, the hot heat source (e.g the exhaust gases from the turbine) heats up the mixture of water and lithium bromide, which separate when evaporating. The as-generated vapor then flows through the condenser where it comes back to the liquid form before entering the lamination valve that brings it to the suitable low pressure to proceed with the evaporation process. The water then enters the evaporator, where it is sprayed on the *chilled water coils* that cause it to evaporate. The evaporation subtracts thermal energy to the water running inside the coils that is thus cooled down (this was the scope of the whole cycle). The so obtained vapor finally passes through the absorber where the original concentration of the two substances is restored. In fact, the property of the LiBr of attracting the molecules of water vapor is what allows the evaporation process to occur at a low enough pressure. The regenerated mixture is then pumped to the generator to restart the cycle. It must be specified that a separated loop, working in the opposite direction of the one described above, exists between generator and absorber. This loop is in charge of taking the fluid with a high concentration of LiBr in the generator to the absorber to make the regeneration process possible.

The system here described is representative of a *single-stage absorption chiller*; more complex systems, requiring the addition of a few steps, are commercially available and are referred to as *double-stage absorption chillers*. As already done with the electric chillers, the efficiency of this systems is here analyzed by calculating the coefficient of performance that can, in this case, have a different definition. In fact, the COP defined for the electric chiller considered the work done on the cycle at the denominator. For absorption chillers, this definition can be, so that a COP defined as thermal is introduced instead:

$$COP_t = \frac{Q_-}{Q_+} \tag{5.2}$$

- Q_- Heat removed from the cold source;
- Q_+ Heat transferred from the hot source to the generator.

The values for the thermal COP for a *single-stage absorption chiller* average between 0.6 and 0.8[12], much lower than the typical values for an *electric chiller* that range from 4.0 o 8.0. *Double stage* absorption chillers could lead to slightly better results (COP_t from 1.0 to 1.2) but, as anticipated, they will not be treated.

5.2 eQuest ® Absorption chiller model

The implementation of a completely new model for the absorption chiller on eQuest® is not one of the objectives of this study, however, a model needs to be implemented to obtain the necessary data to proceed with the TES analysis. In this section are thus discussed the main parameters and performance curves required by the software, as well as the improvements already made by Cicciarella and Romano in their studies [7][12]. Before defining the curves, the definitions of *chilled water temperature* (CWT) and *condenser temperature* are provided for the sake of clarity. The chilled water temperature represents the temperature of the water flowing inside the *cooling coils* that is thus set by the user according to the set-point temperature desired. The condenser temperature, instead, depends on the outdoor temperature.

The curves required by eQuest when defining a *single effect absorption chiller* are the following[11]:

- *Percentage capacity* with respect to the *chilled water temperature*: this one represents the fraction of cooling capacity available and can be calculated as the ratio between the actual capacity and the design capacity;
- *Percentage COP* with respect to the *chilled water temperature*: again, this represents the ratio of the COP in the current condition over the design one;

- *COP* with respect to the *condenser temperature*;
- *Percentage capacity* with respect to the *condenser temperature*;
- *Percentage COP* as a function of the *PLR*.

All of the upgrades performed on the eQuest® native model, used as a reference the data and specifications from the YORK® chiller model *Millennium YIA*^{TM} [23][24].

5.2.1 Chilled water temperature effect

The temperature of the chilled, as intuitive, has a strong influence on the performances of the chiller, as even a small reduction negatively affects the evaporation capacity. This is due to the fact that the lower the temperature of the evaporating source, the harder it is to cause the fluid to evaporate because the evaporation temperature decreases.

The curves that describe this behaviour are reported below respectively for the eQuest model and the upgraded one and are graphically represented in Figure 32; in both curves, x represents the *chilled water temperature*.

$$Cap_{\%eQuest} = -0.089x^2 + 10.247x - 177.261 \tag{5.3}$$

$$Cap_{\%YORK} = -0.089x^2 + 9.357x - 138.943 \tag{5.4}$$

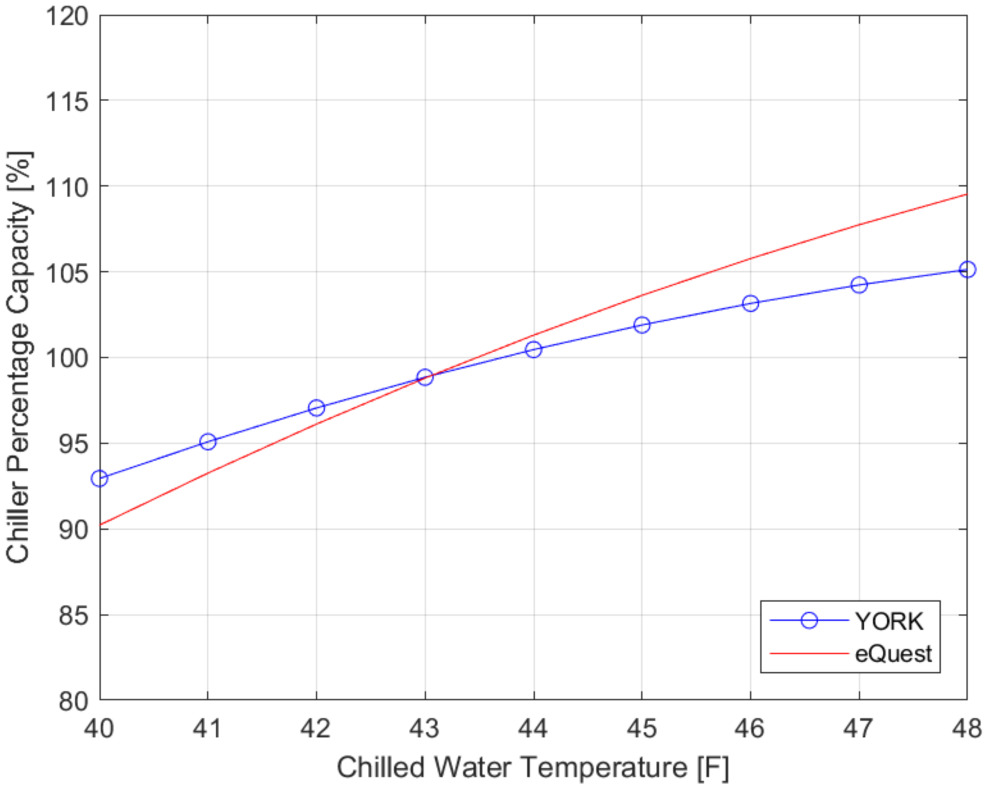

Figure 32: Percentage Chiller Capacity as a function of the Chilled Water Temperature

Equation 5.4 is not provided by the manufacturer; it is instead obtained by knowing the relationship between the *chilled water temperature* and the percentage of fuel consumption. By plotting these two curves, it possible to notice that a capacity of 100% can be reached if the CWT is 44[F] and the condenser temperature is kept constant at 85[F]. These results are not accidental, but come from the ARI 550/590 standard [25] that imposes a CWT of 44[F] and a condenser temperature of 85[F], therefore, both curves are normalized according to these values. The main difference that can be observed concerns the slope of the curves: the YORK® one has a reduced steepness compared to native model, meaning that the CWT has a smaller effect on the cooling capacity.

The next curve, function of the CWT, required by eQuest®, describes the trend of the percentage COP. This one can be easily obtained knowing both the percentage capacity and fuel consumption.

$$COP_{\%} = \frac{COP}{COP_{des}} = \frac{\frac{\text{Cooling Capacity}}{\text{Fuel Consumption}}}{COP_{des}} = \frac{\frac{\text{Cool. Cap}_{des} \cdot Cap_{\%}}{\text{Fuel Cons.}_{des} \cdot \text{Fuel Cons}_{\%}}}{COP_{des}} = \tag{5.5}$$

$$COP_{\%} = \frac{COP_{des} \cdot \frac{Cap._{\%}}{\text{Fuel Cons.}_{\%}}}{COP_{des}} = \frac{Cap._{\%}}{\text{Fuel Cons.}_{\%}} \tag{5.6}$$

Using Equation 5.6 the following curve is obtained and represented in Figure 33:

$$COP_{\% YORK} = -0.093x^2 + 10.518x - 183.526 \tag{5.7}$$

The eQuest® model, instead considers the COP in a certain condition to be constantly equal to 65% of the design one.

$$COP_{\% eQuest} = 65 \tag{5.8}$$

In the following analysis, the CWT imposed by the user is assumed to be kept constant at 44[F], so that the curve follows the ARI 550/590 standard, showing a cooling capacity and COP equal to 100% at 44[F].

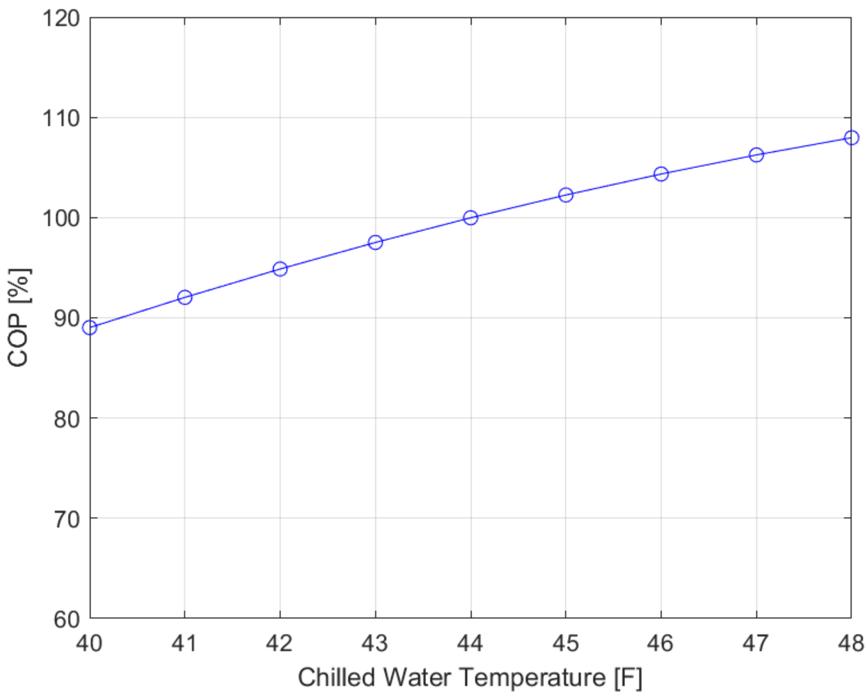

Figure 33: Percentage COP as a function of the Chilled Water Temperature

5.2.2 Condenser temperature effect

The first curve that investigates the influence of the condenser temperature, requires to describe the relationship between this one and the percentage COP. In this case, however, the equation is provided by the manufacturer:

$$COP_{\%YORK} = 0.011x^2 - 2.68x + 243.835 \tag{5.9}$$

Where x represents the *condenser temperature.* The standard used is, once again, the ARI 550/590, according to which a COP of 100% is reached when the condenser temperature is 85 [F]. Equation 5.9 is represented in Figure 34.

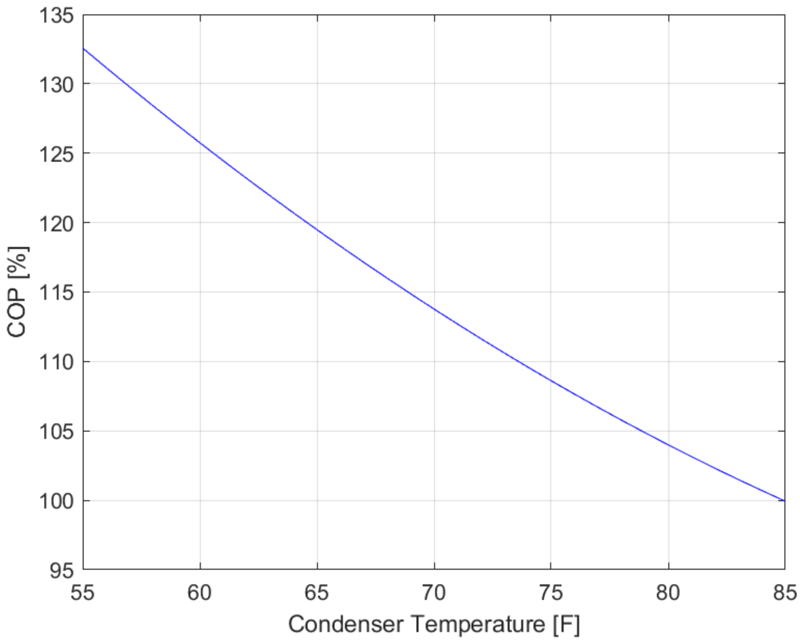

Figure 34: Percentage COP of the chiller as a function of the Condenser Temperature

eQuest® also needs the relationship between COP and condenser temperature, as well as the percentage cooling capacity. These curves are reported below in Equation 5.10 to 5.12 and in Figure 35 and Figure 36.

$$COP_{eQuest} = -(2E-5)x^2 - (3E-3)x + 1.054 \tag{5.10}$$

$$COP_{YORK} = (9E-5)x^2 - 0.021x + 1.898 \tag{5.11}$$

$$Cap_{\%YORK} = -(1E-3)x^2 - 0.692x + 165.928 \tag{5.12}$$

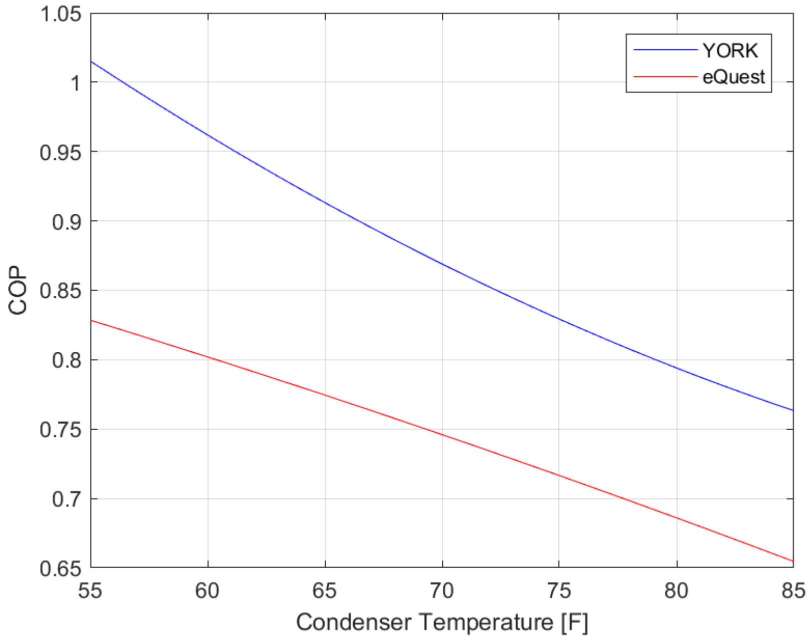

Figure 35: COP of the chiller as a function of the Condenser Temperature

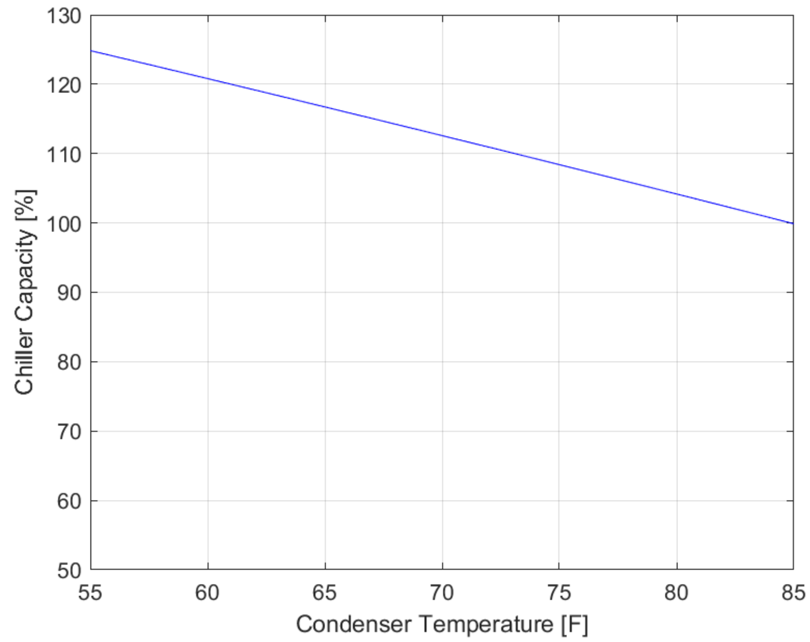

Figure 36: Capacity of the chiller as a function of the Condenser Temperature

5.2.3 Partial Load operation

The last situation to evaluate is the operation at partial load condition; in fact, just like for the turbine, the behaviour of the chiller when it is not running at full capacity tends to change. The absorption chiller here modeled, is fed by the *recoverable heat* produced by the turbine, however, since the prime mover works using a FEL management strategy, the amount of thermal energy available will change throughout the year and will not be guaranteed all the time. Moreover, the facility cooling demand is variable as well. As a consequence of that, it is critical to model a chiller that shows optimal performances even at partial load. The relationships, describing both the eQuest model and the improved one, elaborated by Cicciarella [7] are reported in Equation 5.13 and 5.14 and in Figure 37, where x represents the PLR.

$$COP_{eQuest} = (6E - 5)x^2 + (1E - 3)x + (3E - 5) \tag{5.13}$$

$$COP_{YORK} = -(3E - 5)x^2 + (4E - 3)x + 0.587 \tag{5.14}$$

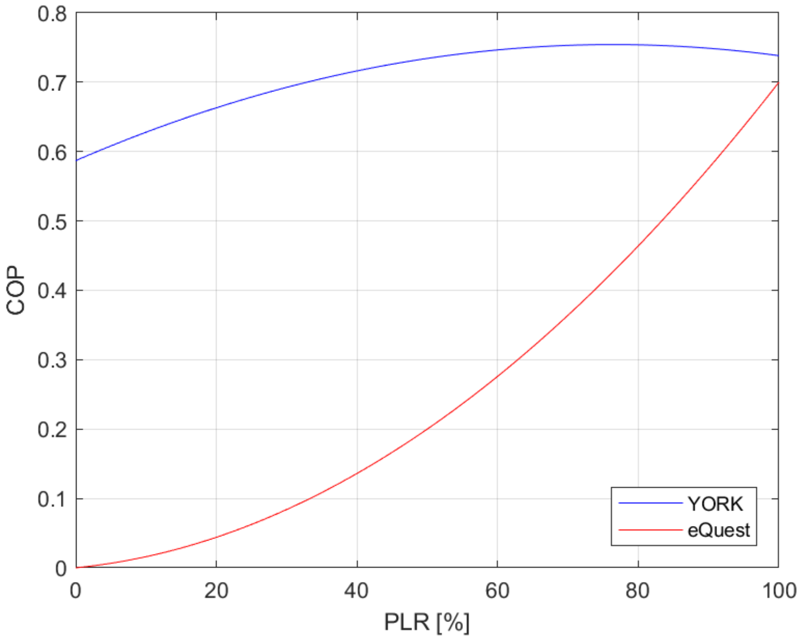

Figure 37: COP of the chiller as a function of the Partial Load Ratio for the YORK and the eQuest models

5.3 CCHP Plant layout

The combined cooling, heat and power plant layout is obtained starting from the cogeneration system already modeled, therefore all the considerations made and the energy fluxes defined, remain valid. The fundamental modification consists in the addition of the *absorption chiller* in the *Space Cooling Water Loop*. The layout of the plant, as shown in eQuest®, is reported in Figure 38.

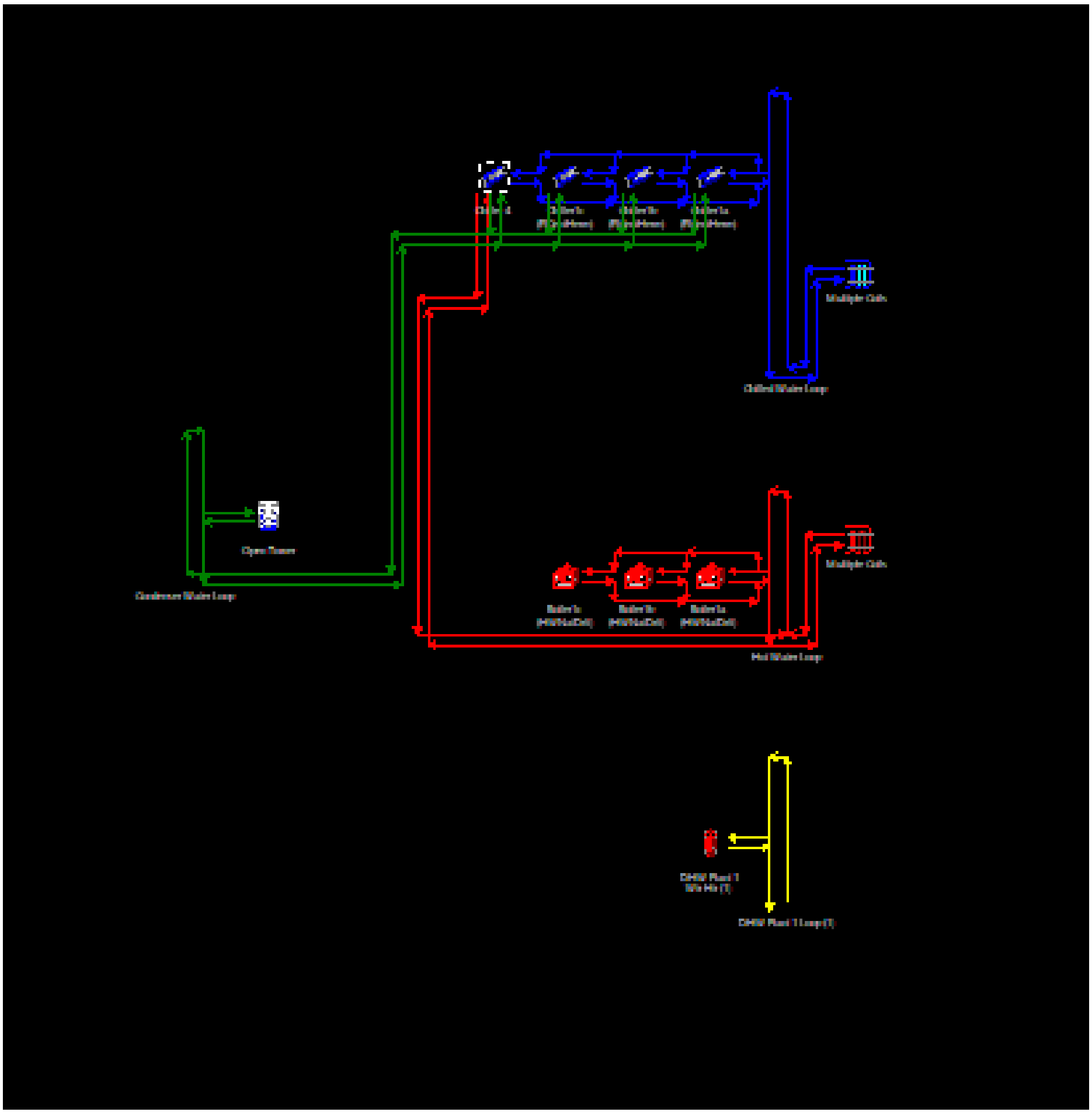

Figure 38: CCHP System representation on eQuest

Since the starting point is the CHP system modeled in Section 3, the prime mover is the same SOLAR® turbine. The absorption chiller is connected to three circulation loop:

- **Hot water loop:** from this loop, the chiller receives the high-temperature thermal energy needed to run;
- **Chilled water loop:** the water flowing inside this loop is the water that has to be cooled down by the chiller, hence the heat source that causes the refrigerant to evaporate;
- **Condenser water loop:** this loop is used to discharge the thermal energy generated throughout the process.

The electric chiller works as a backup for those cases where the *absorption chiller* is not able to cover the entire cooling demand because the *recovered heat* is not sufficient. To allow the system to run by prioritizing the exploitation of the *absorption chiller* instead of the electric one, a control system was implemented.

When implementing the CCHP system on eQuest® a capacity for the chiller has to be determined in order to make a wide exploitation of the WRH possible. The turbine sizes vary from 500[kW] to 1300 [kW], just like in Chapter 3. However, the sizing of the system resulted much more complex in this case, because eQuest®, despite the equipment control implemented, was not able to correctly manage the *absorption chiller*, causing the boiler to run in order to make the chiller work when the *recovered heat* was not sufficient. What was meant to happen, instead, is that, in lack of *recoverable heat*, the electric chillers have the priority, so that the *absorption* one only runs when some exhaust heat is available. As a consequence of that, the fuel consumption from the boilers rose significantly. To ensure the proper operation of the entire system (in a way that does not negatively affect its efficiency) the *absorption chiller* has to be sized according to the amount of *recoverable heat* available, so that it runs until the heat is fully exploited and turned into *recovered heat*. After that, the electric chillers start to work to cover the remaining part of the load.

In order to find a correct size of the *absorption chiller*, that would not imply the issues explained above, an empirical procedure was adopted, consisting in analyzing both the *recoverable heat* and the boilers gas consumption. The size of the chiller was chosen by finding a trade-off between the maximum value of WRH in summer and the increase in fuel consumption. This means that the size chosen was the best possible, in the range from the minimum and maximum WRH, that would not cause the boilers consumption to rise. The results obtained are summarized in Table VI. However, some increase in the gas consumption always occurs so, in order to avoid this problem, the following analysis will be more carefully developed in Excel.

TABLE VI: **ABSORPTION CHILLER CAPACITY**

Turbine size [kW]	Chiller capacity [MMBtu/h]
500	1.0
600	1.8
700	2.7
800	3.2
900	3.6
1000	4.0
1100	4.5
1200	5.0
1300	5.8

5.4 Integration of the Thermal Storage in the Trigeneration system

In this section the model of a high-temperature energy storage is added to the *combined cooling, heat and power system* in order to determine, whether it impacts on the overall performances of the plant.

Similar to what was done in Chapter 4, an Excel spreadsheet was implemented to describe the charge and discharge dynamics of tank; this time, however, the thermal load considered, also accounted for the heat needed to run the generator in the *absorption chiller*. A block diagram is provided in Figure 39 to explain which data data come from eQuest ® and what are the results available after the Excel elaboration.

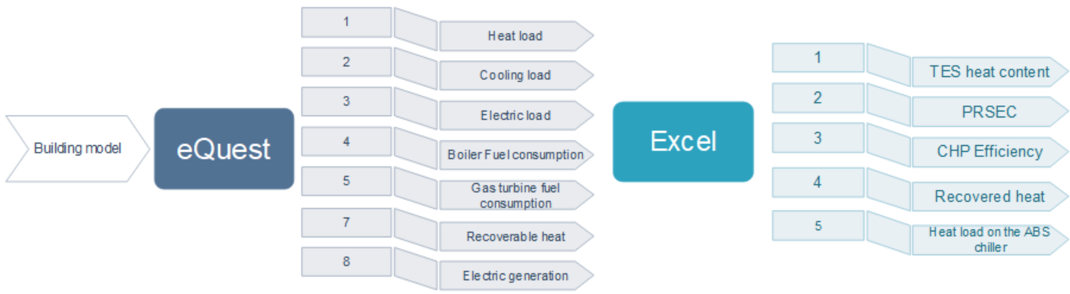

Figure 39: eQuest and Excel Block Diagram

The considerations made in Chapter 4 concerning the thermal losses and the benefits of the TES remain valid. Furthermore, in the trigeneration case, the idea of introducing a thermal storage is, supposedly, even more convenient. In fact, one of the results obtained in Chapter 4, was a poor exploitation of the storage in the summer months, due to a large excess of *recoverable heat* compared to the thermal demand. The introduction of an *absorption chiller*, makes the heat load rise even in summer, hence the TES could have a beneficial effect on the operation of the system, helping balancing the fluctuations and further avoiding the use of the electric chillers.

5.4.1 The Excel model

The Excel model for the CCHP system exploits the same base concepts of the one implemented for the CHP system, but requires the addition of some elements. As anticipated in the previous section, the eQuest® model does not correctly prioritize the operation of the chillers and their sources, so the Excel model was built so that the equipment is properly controlled. The first step was to determine the thermal energy needed to feed the *absorption chiller*. Knowing the hour-by-hour load on the cooling coils, the desired values are obtainable exploiting the COP_t equation (COP_t=0.75) dividing the the cooling load by the COP_t. Figure 40 shows the facility thermal demand when also accounting for the *absorption chiller*.

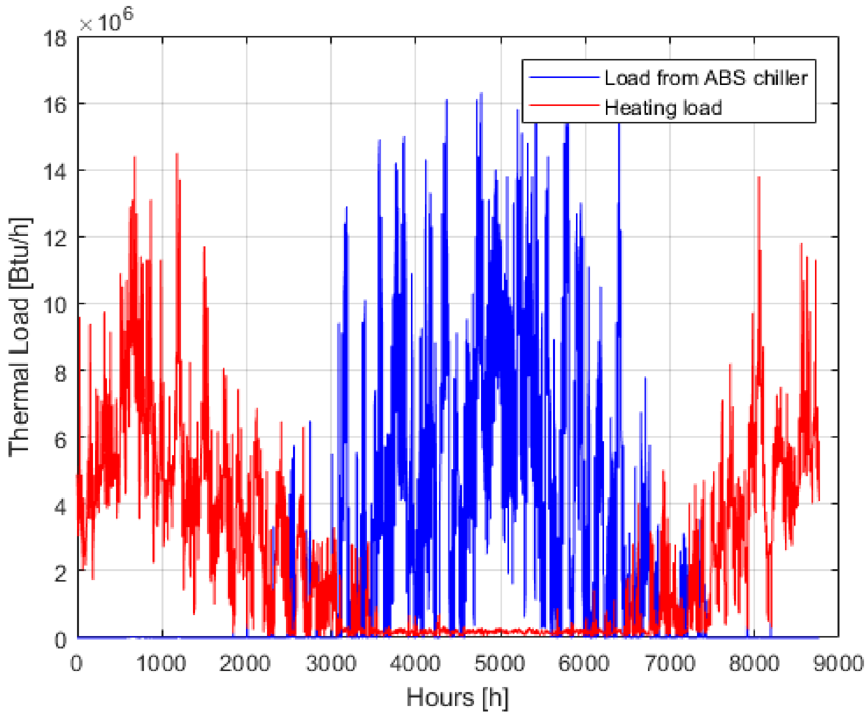

Figure 40: Facility thermal load from space heating and ABS chiller

The *recovered heat* and the performance indexes, as well as the dynamic of the storage are calculated with the same strategy already implemented for the CHP plant, while the new electric load and the prime mover electric production are obtained from eQuest® after confirming their reliability. Finally the boilers fuel consumption was left unchanged since, according to the control strategy chosen, the *absorption chiller* has to work only if fed by exhaust heat, thus it does not have to cause the gas consumption to grow.

5.4.2 The sizing process

The sizing process for the CCHP system, follows the same iterative approach used for the cogeneration plant. In the first step a TES capacity of 4 [MMBtu] is kept unvaried while the gas turbine size ranges from 500 [kW] to 1300 [kW]. The CHP efficiency and the PRSEC are calculated in order to find an optimal size for the prime mover. The results are summarized in Table VII.

TABLE VII: **CCHP SYSTEM PERFORMANCES AS A FUNCTION OF THE TURBINE SIZE**

Turbine size [kW]	**PRSEC** [%]	η_{CHP} [%]
500	20.20	81.81
600	22.34	78.05
700	23.88	72.48
800	23.98	70.37
900	22.07	64.33
1000	19.49	60.60
1100	16.18	57.08
1200	12.61	53.88
1300	7.71	50.63

It is possible to notice that the 800[kW] turbine is again the best choice. Furthermore, both the PRSEC and the efficiency values are higher compared to the equivalent CHP system. This result comes from a better exploitation of the *exhaust heat*, but also from a slightly wider use of the storage, especially in the summer months.

The second iteration sets the turbine size to 800 [kW] and has the tank capacity vary from 0 to 100 [MMBtu]. The results are graphically shown in Figure 41 and Figure 42.

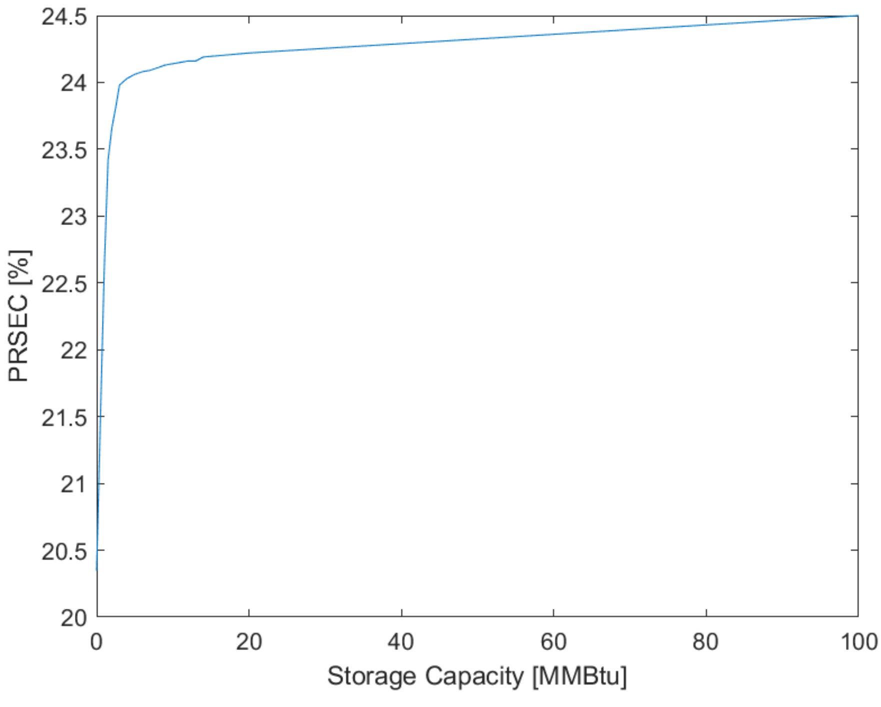

Figure 41: Second iteration: PRSEC as a function of TES Capacity

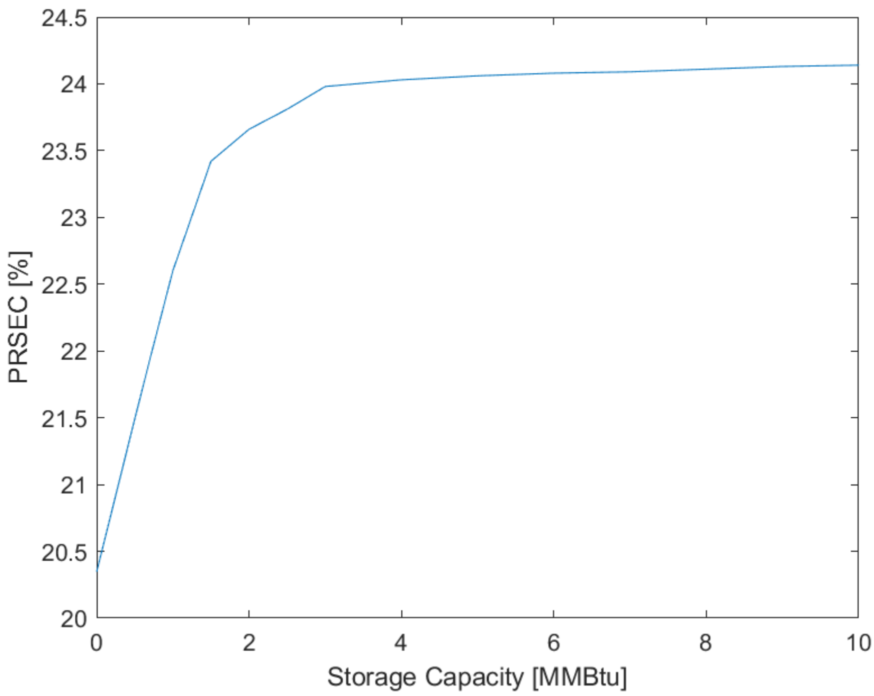

Figure 42: Enlargement of the PRSEC trend as a function of TES Capacity (from 0 to 10 MMBTU)

Once again, the results show an increasing trend of the PRSEC as a function of the TES Capacity. However, a significant improvement in the system performances can be noticed when adding a relatively small tank up to 4 [MMBtu]; after that an even strong increase in the storage capacity does not result in an equivalent improvement in the performances, that remain stable at around 24%. It can thus be concluded that, to reach a PRSEC value of 24%, a Thermal Energy Storage with a capacity of 4 [MMBtu] (around 16,500 [gal]) could be an effective choice.

CHAPTER 6

CONCLUSION

This study analyses the performances of four plant layouts for a large health care facility located in Chicago. The first two options were represented by a Cogeneration system and a Trigeneration system, while the last two were based on them and improved by implementing a High-Temperature Thermal Energy Storage. The prime mover used in all four cases was a combustion turbine, whose exhaust gases were recovered to satisfy part of the heat load of the building for the cogeneration cases, and also part of the cooling demand for trigeneration (where the heat is used to run an absorption chiller). In order to achieve this goal, the CHP and CCHP systems were modeled, using the DOE software eQuest®, on the preexisting model of the hospital developed by the National Renewable Energy Laboratory[3]. On the other hand, since eQuest® often provided poor results, due to some inner limitations when dealing with CHP and CCHP systems, to guarantee a degree of accuracy, part of the model was manually developed on Excel.

The main objective of this work was to assess the influence of the Thermal Energy Storage on the system; this was done by evaluating a parameter called *Percentage Reduction in Source Energy Consumption* (PRSEC). The PRSEC quantifies the relative amount of source energy saved, compared to the base model that is designed to cover its electric load by purchasing all the electricity from the grid and its thermal load by producing hot water with a natural gas boiler.

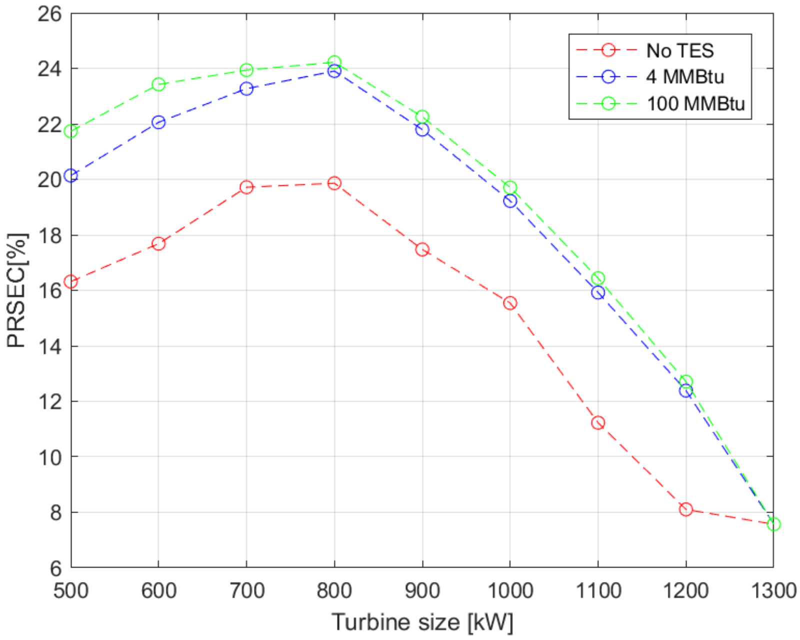

Figure 43: PRSEC vs Turbine size for the cogeneration system

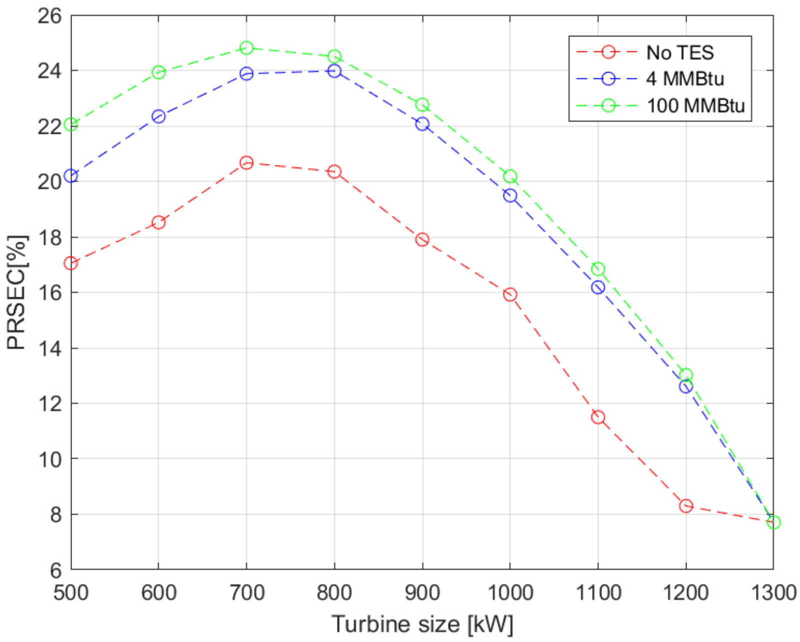

Figure 44: PRSEC vs Turbine size for the trigeneration system

The analysis consisted in finding an optimal size for the prime mover, which was found to be 800 [kW] in all cases, and then a suitable capacity, providing a good trade-off between cost and performances, for the storage tank. Figure 45 and Figure 44 show two family of curves representing the trend of the PRSEC as a function of the turbine size, for three cases each: cogeneration without storage, cogeneration with a 4 [MMBtu] and a 100 [MMBtu] storage and same for trigeneration. It can be noted that the optimal turbine size is always 800 [kW]. However, the most valuable result is given by the conclusion that a big increase in storage capacity does not produce an equal benefit on the plant performance. On the other hand, introducing a relatively small tank, highly affects the behaviour of the system, increasing the PRSEC of around 4%. The exact results, comparing the PRSEC and the recovered heat in the four scenarios, are reported in Table VIII (in all four cases only the optimal solution is chosen).

TABLE VIII: **PERFORMANCES OF THE FOUR PLANT CONFIGURATIONS**

Plant layout	**PRSEC [%]**	Q_{rec}**[MMBtu]**
CHP	19.9	19,201
CHP+TES	23.9	19,296
CCHP	20.3	32,532
CCHP+TES	24.0	32,812

The first thing that can be noted is that trigeneration allows to recover almost twice the amount of heat, compared to cogeneration, and that is due to a better exploitation of the *recoverable heat* in summer months, provided by the introduction of the absorption chiller.

One other major result is that the addition of the storage leads to similar values in both the cogeneration and trigeneration case (a graphic representation is provided in Figure 45). This means that the contribution of the storage is not, as it was expected instead, sensibly wider when adding the absorption chiller. A possible reason might rely in the morning peaks of the cooling demand that quickly discharge the tank, requiring, then, many hours to charge it again.

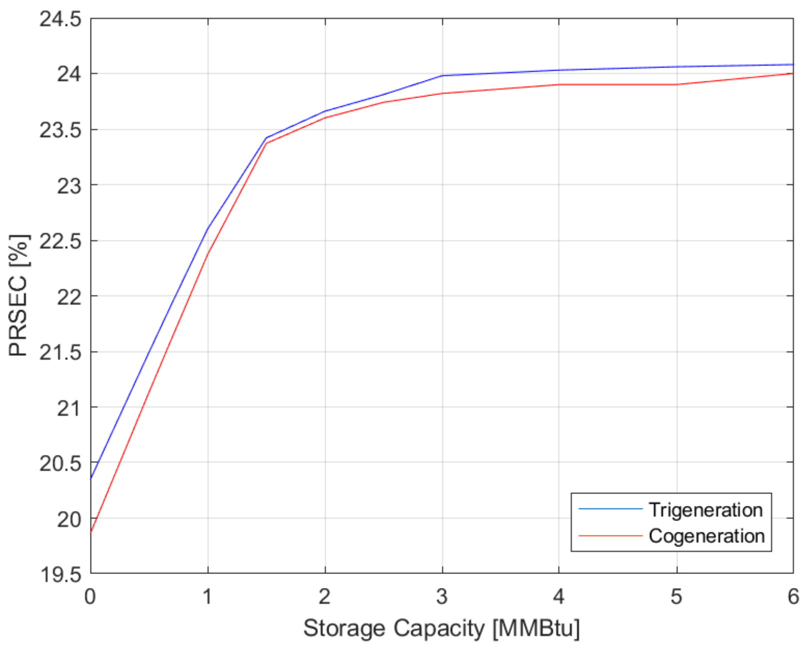

Figure 45: PRSEC vs TES Capacity for the CHP and CCHP systems

The final important result, on the other hand, is that, introducing a small thermal storage (in the order of 4 to 6 [MMBtu]) in a CHP or CCHP plant, for this kind of facilities, enables a much larger improvement in the overall performances than a bigger turbine would. This results is extremely advantageous from the economic point of view, in fact, water storage tanks (especially if not pressurized) are tens of times cheaper than large turbines. Also, they are easier to operate and maintain and, finally, allow not to oversize the turbine so that it can run full load for most of the time.

CITED LITERATURE

1. Haefke, C. & Cuttica, J. Market sector fact sheet: Combined heat and power in hospitals. *US DOE CHP Technical Assistance Partnership* (2013).

2. Bourgeois, T., Dillingham, G., Panzarella, I. & Hampson, A. Combined heat and power: Enabling resilient energy infrastructure for critical facilities. *ICF International Paper* (2013).

3. Bonnema, E., Studer, D., Parker, A., Pless, S. & Torcellini, P. *Large hospital 50% energy savings: Technical support document* tech. rep. (National Renewable Energy Lab.(NREL), Golden, CO (United States), 2010).

4. ANSI/ASHRAE. Standard 90.1-2004, Energy standard for buildings except low rise residential buildings. *American Society of Heating, Refrigerating and Air-Conditioning Engineers, Inc* (2004).

5. ASHRAE. Standard 169-2006: Weather Data for Building Design Standards. *American Society of Heating, Refrigerating, and air-conditioning Engineers, Inc., Atlanta, GA* (2006).

6. Crinò, A. *CHP Technologies in the Midwest of USA: Energy and Economic Evaluation of a CHP System* PhD thesis (2014).

7. Cicciarella, F. *Simulation of Emerging Smaller-Scale Tri-Generation Systems* PhD thesis (2015).

8. Hunt, R. The history of the industrial gas turbine (part 1 the first fifty years 1940-1990). *Power Engineer* **15** (2011).

CITED LITERATURE (Continued)

9. Galli, P. *Simulation of a Small Scale Co-generation System Using a Microturbine* PhD thesis (2016).
10. *Gas Turbines M701J Series* ://www.mhps.com/products/gasturbines/lineup/m701j/.
11. Hirsch, J. *et al.* eQuest® user manual: topics. *Building Energy Use and Analysis Program* **3** (2006).
12. Romano, L. *Development of Simulation Techniques for Thermal Storage Coupled to Co-generation/Trigeneration Systems* PhD thesis (2018).
13. *Solar Turbine: Turbomachinery systems for oil and gas application* https://mysolar.cat.com.
14. *Solar turbine: product support* https://mysolar.cat.com.
15. ISO. ISO 3977-2: Gas turbines-part 2: Standard reference conditions and ratings (1997).
16. EPA. Catalog of CHP Technologies. *The U.S. Environmental Protection Agency: Washington, DC, USA* (2015).
17. ANSI/ASHRAE. Standard 105-2014: Standard Methods of Determining, Expressing and Comparing Building Energy Performance and Greenhouse Gas Emissions. *American Society of Heating, Refrigerating and Air-Conditioning Engineers, Inc* (2014).
18. Celador, A. C., Odriozola, M. & Sala, J. Implications of the modelling of stratified hot water storage tanks in the simulation of CHP plants. *Energy Conversion and Management* **52** (2011).
19. *Highland Tanks:ASME Pressure Vessels Water Storage Tanks* https://www.highlandtank.com.
20. *Average costs for water tanks* https://www.improvenet.com/r/costs-and-prices/water-or-fuel-tank-replacement-cost.

CITED LITERATURE (Continued)

21. Al-Sulaiman, F. A., Hamdullahpur, F. & Dincer, I. Trigeneration: a comprehensive review based on prime movers. *International journal of energy research* **35,** 233–258 (2011).

22. Venkatarathnam, G. & Murthy, S. S. Refrigerants for vapour compression refrigeration systems. *Resonance* **17,** 139–162 (2012).

23. *YORK: Millennium yia single-eect absorption chillers* http://www.johnsoncontrols.com/.

24. *YORK: Isoflow single-eect absorption chillers* http://www.johnsoncontrols.com/.

25. ARI. Standard ARI: 550/590-2003. Performance rating of water-chilling packagesusing the vapor compression cycle. *Air-conditioning and Refrigeration Institute* (2003).

VITA

NAME	Claudia Puglisi
EDUCATION	Master of Science in Mechanical Engineering University of Illinois at Chicago, USA, August 2019 Master of Science in Energy and Nuclear Engineering Politecnico di Torino, Italy, July 2019 Bachelor of Science in Energy Engineering Politecnico di Torino, Italy, October 2017
HONORS	TOP-UIC mobility scholarship for Double Degree program, 2018-2019 Thesis under request scholarship, 2018-2019